YITP-11-14
TIT/HEP-610
UTHEP-623

g-functions and gluon scattering amplitudes at strong coupling

Yasuyuki Hatsuda*, Katsushi Ito†, Kazuhiro Sakai‡ and Yuji Satoh§

*Yukawa Institute for Theoretical Physics, Kyoto University
Kyoto 606-8502, Japan

†Department of Physics, Tokyo Institute of Technology
Tokyo 152-8551, Japan

‡Research and Education Center for Natural Sciences
and Hiyoshi Department of Physics, Keio University
Yokohama 223-8521, Japan

§Institute of Physics, University of Tsukuba
Ibaraki 305-8571, Japan

Abstract

We study gluon scattering amplitudes/Wilson loops in $\mathcal{N} = 4$ super Yang–Mills theory at strong coupling by calculating the area of the minimal surfaces in AdS_3 based on the associated thermodynamic Bethe ansatz system. The remainder function of the amplitudes is computed by evaluating the free energy, the T- and Y-functions of the homogeneous sine-Gordon model. Using conformal field theory (CFT) perturbation, we examine the mass corrections to the free energy around the CFT point corresponding to the regular polygonal Wilson loop. Based on the relation between the T-functions and the g-functions, which measure the boundary entropy, we calculate corrections to the T- and Y-functions as well as express them at the CFT point by the modular S-matrix. We evaluate the remainder function around the CFT point for 8 and 10-point amplitudes explicitly and compare these analytic expressions with the 2-loop formulas. The two rescaled remainder functions show very similar power series structures.

February 2011

*hatsuda@yukawa.kyoto-u.ac.jp
†ito@th.phys.titech.ac.jp
‡sakai@phys-h.keio.ac.jp
§ysatoh@het.ph.tsukuba.ac.jp

1. Introduction

It has been recognized that there exists an integrability structure in gluon scattering amplitudes in $\mathcal{N} = 4$ super Yang–Mills theory at strong coupling. Gluon scattering amplitudes are dual to the Wilson loops made of light-like segments [1, 2]. By using the AdS-CFT correspondence, the amplitudes at strong coupling are shown to be equal to the area of the minimal surface in AdS with the same null polygonal boundary [1]. For $n(\geq 6)$-point amplitudes [3, 4] they are shown to differ from the Bern-Dixon-Smirnov (BDS) conjecture [5]. The deviation from the BDS conjecture is called the remainder function, which is a function of the cross-ratios of the external gluon momenta.

It has been found that the equations for the minimal surface reduce to the Hitchin system and the area of the surface is determined by the Stokes data of its solutions [6–9]. The Stokes data and their cross-ratios obey the functional equations called the T-system [10] and the Y-system [11]. The area of the minimal surface is determined by the thermodynamic Bethe ansatz (TBA) equations [12] associated with the Y-system [8].

Y-systems are closely related to two-dimensional integrable models. For the 6-point gluon scattering amplitude, which corresponds to the minimal surface with a hexagonal null boundary in AdS_5, the related Y-system and the TBA equations are those of the $\mathbb{Z}_4$-symmetric integrable model [7]. In our previous paper [13], we solved the TBA equations with chemical potential by the integrable perturbation of conformal field theory (CFT) and evaluated the free energy. In order to obtain the analytic form of the remainder function near the CFT point corresponding to the regular polygonal Wilson loop, it is moreover necessary to calculate small mass expansion of the Y-functions, which was determined numerically in [13].

A key observation for computing the Y-functions analytically is as follows: The TBA free energy is obtained from the partition function on a cylinder with the periodic boundary condition. We can also consider the free energy on a cylinder with different boundary conditions. Affleck and Ludwig [14] introduced the g-functions from this free energy, which count the ground state degeneracy of the system with boundaries (the boundary entropy). In [15, 16], Dorey et al. studied the exact off-critical g-functions for the purely elastic scattering theory and derived the integral equation for them. They evaluated the g-functions using the integrable perturbation of the boundary CFT. Remarkably, ratios of the g-functions obey the same integral equations for the T-functions. This enables us to obtain the analytic expression

for the Y-functions from the g-functions and determine the analytic form of the remainder function near the CFT point.

In this paper, we study the remainder function for $2\tilde{n}$-point gluon scattering amplitudes at strong coupling, which correspond to minimal surfaces in AdS_3 with a $2\tilde{n}$-gonal light-like boundary. This corresponds to the case where the gluon momenta are in $\mathbb{R}^{1,1}$. In [9] the related integrable system was shown to be the homogeneous sine-Gordon model (HSG) [17] with purely imaginary resonance parameters. The relevant CFT is the generalized parafermions $\mathrm{SU}(\tilde{n}-2)_2/\mathrm{U}(1)^{\tilde{n}-2}$ [18]. In this paper we will study the boundary and bulk perturbation of the generalized parafermions and calculate the ratios of the g-functions. For the octagon ($\tilde{n}=4$) and the decagon ($\tilde{n}=5$), we will calculate the perturbative corrections to the T-/Y-functions, the free energy and the remainder function explicitly. We compare these analytic expressions of the remainder function with the 2-loop formulas proposed in [19–21] around the CFT limit.

The above analytic results are important to understand the structure and the momentum dependence of the amplitudes at strong coupling exactly. The purpose of this paper is to take a step toward this direction by analyzing the TBA system near the CFT point from the conformal perturbation theory (CPT). A point in our discussion is that not only the free energy but also the Y-functions can be discussed in this framework owing to the relation between the T-/Y-functions and the g-functions.

This paper is organized as follows. In section 2, we review the TBA system for the minimal surfaces in AdS_3. In section 3, we discuss the HSG model and the free energy for the integrable bulk perturbations. In section 4, we study the HSG model from the CPT of the generalized parafermions and the relation between the T-functions and the g-functions. In section 5, we investigate the small mass expansions of the g-function and the remainder function for the octagon. In section 6, we argue the corrections to the free energy, the T-/Y-functions and the remainder function for the decagon. In section 7, we compare the analytic expressions for the remainder functions for the octagon and the decagon with the 2-loop results. In section 8, we give a summary and a discussion. In Appendix A, we present the high-temperature expansion of the g-function for the Ising model in detail. In Appendix B, we study the CPT of an SU(2) coset model with fractional level. In Appendix C, we discuss the expansion of the Y-functions in the case of complex masses. In Appendix D, we examine the structure of the expansion of the remainder functions at higher orders.

2. Review of TBA system for minimal surfaces in AdS_3

2.1. Problem

Gluon scattering amplitudes at strong coupling are evaluated by the area of minimal surfaces in AdS_5 [1]. The minimal surfaces have a polygonal boundary located on the AdS boundary. Each edge of the polygonal boundary represents a gluon momentum. Throughout this paper we consider the case where the minimal surfaces stretch inside the maximal AdS_3 subspace. In this case, the polygonal boundary is contained inside $\mathbb{R}^{1,1}$ at the AdS boundary. Namely, we consider amplitudes with all the gluon momenta being restricted in $\mathbb{R}^{1,1}$. For general $2\tilde{n}$-point amplitudes, we label the vertices of the polygon in the light-cone coordinates as $x_{2k-1} = (x_k^+, x_k^-),\ x_{2k} = (x_{k+1}^+, x_k^-),\ k = 1, \ldots, \tilde{n}$ (with identification $x_{\tilde{n}+1}^{\pm} = x_1^{\pm}$). The gluon momenta are then given by $x_j - x_{j+1},\ j = 1, \ldots 2\tilde{n}$ ($x_{2\tilde{n}+1} = x_1$). These data completely fix the shape and the area of the minimal surfaces.

As the gluon scattering amplitudes in $\mathcal{N} = 4$ SYM are infrared divergent, the area of the minimal surfaces are also divergent. Nevertheless, the structure of the divergence has been well studied and one can read off meaningful results after specifying an appropriate regularization scheme. The finite results are commonly analyzed in the form of the remainder function, namely the deviation of the area from the conjecture of Bern, Dixon and Smirnov [5]. It is a dual-conformally invariant quantity and hence a function of cross-ratios of x_j. The form of the function is of our central interest.

2.2. T-/Y-system and TBA equations

Despite the difficulty in analytically constructing the minimal surfaces for general polygonal boundaries, it turned out that the area can be computed by solving TBA type integral equations. This subsection is devoted to a brief summary of the TBA equations and the associated T-/Y-system for the minimal surfaces in AdS_3. For details, see [6, 8, 9, 22].

The standard procedure to analyze the minimal surfaces in AdS_3 is to consider the auxiliary linear problem associated with the original nonlinear equations of motion. For any minimal surface in AdS_3 one can consider SU(2) Hitchin equations [6], which are a set of first order linear differential equations defined on the world-sheet with coordinates $z, \bar{z}$. To be precise, there appear two sets of Hitchin equations corresponding to $\mathrm{SL}(2)_{\mathrm{L}}$, $\mathrm{SL}(2)_{\mathrm{R}}$ evolutions of AdS_3. These are promoted to a one-parameter family of differential equations with a spectral parameter ζ, where $\zeta = 1$

and $\zeta = i$ correspond to the original $\mathrm{SL}(2)_{\mathrm{L}}$ and $\mathrm{SL}(2)_{\mathrm{R}}$ cases, respectively. The minimal surface is constructed as the product of the solutions of these Hitchin equations.

When the minimal surface possesses a $2\tilde{n}$-gonal boundary, solutions of the Hitchin equations exhibit the Stokes phenomena. The world-sheet is divided, with respect to the asymptotic behavior of solutions, into $\tilde{n}$ angular regions called the Stokes sectors. When moving from one sector to another at large $|z|$, a solution shows drastic change in its asymptotic behavior. This corresponds to moving from one cusp to another cusp at the boundary of the minimal surface. In each sector one can uniquely (up to normalization) choose the "small" solution, which shows the fastest decay for $|z| \to \infty$ among the solutions. We let $s_j(z, \bar{z}; \zeta)$ denote such small solution in the j-th Stokes sector ($j = 1, \ldots, \tilde{n}$). We are considering (ζ-dependent) SU(2) Hitchin equations, and thus s_j's are 2-component column vectors. We fix the normalization of s_j so that

$$\langle s_j, s_{j+1} \rangle := \det(s_j \, s_{j+1}) = 1. \tag{2.1}$$

Since there are only two linearly independent solutions, all s_j's are expressed as linear combinations of any two of them. The coefficients of these linear combinations are called the Stokes data. The Stokes data are redundant and one finds relations among them. It turned out that such relations are concisely expressed in the form of T-system, where Stokes data are identified with T-functions [8]. In the present case, the T-system reads

$$T_j^+ T_j^- = 1 + T_{j-1} T_{j+1}, \tag{2.2}$$

where $j = 1, \ldots, \tilde{n} - 3$. The T-functions are given by

$$T_{2k+1}(\theta) = \langle s_{-k-1}, s_{k+1} \rangle, \qquad T_{2k}(\theta) = \langle s_{-k-1}, s_k \rangle^+ \tag{2.3}$$

for T_j with $j = 0, \ldots, \tilde{n} - 2$ and the rest are set to be zero. Here we introduced the new variable θ by

$$\zeta = e^{\theta} \tag{2.4}$$

and the convention $f^{\pm} := f(\theta \pm \pi i/2)$. Note that Stokes data are by definition independent of $z, \bar{z}$ and depend only on ζ. In (2.3) there appear s_j with $j \leq 0$, which are defined by successively applying the normalization condition (2.1). As s_j and $s_{j+\tilde{n}}$ correspond to the same Stokes sector, they are, as functions of $z, \bar{z}$, proportional to each other

$$s_j \propto s_{j+\tilde{n}}. \tag{2.5}$$

We see that $T_0 = 1$ and $T_{\tilde{n}-2}$ is equal to one of the proportionality coefficients (monodromies). The present T-system is of the standard $A_{\tilde{n}-3}$ type.

While the T-functions completely characterize the shape of the minimal surface, they contain unphysical gauge degrees of freedom. Instead, one can consider gauge invariant quantities called Y-functions. In this case, they are given by

$$Y_j = T_{j-1}T_{j+1}. \tag{2.6}$$

Note that Y_j with $j = 1, \ldots, \tilde{n}-3$ are in general nontrivial functions while the rest are zero. Y-functions correspond directly to the physical variables. They are essentially the cross-ratios:

$$Y_{2k} = -\mathcal{X}_{-k,k,-k-1,k+1}\,, \quad Y_{2k+1} = -\mathcal{X}^{+}_{-k-1,k,-k-2,k+1}\,, \tag{2.7}$$

where

$$\mathcal{X}_{ijkl} := \frac{\langle s_i, s_j\rangle\langle s_k, s_l\rangle}{\langle s_i, s_k\rangle\langle s_j, s_l\rangle}\,, \tag{2.8}$$

and

$$\mathcal{X}_{ijkl}(\zeta = 1) = \frac{x^+_{ij}x^+_{kl}}{x^+_{ik}x^+_{jl}} =: \chi^+_{ijkl}\,, \quad \mathcal{X}_{ijkl}(\zeta = i) = \frac{x^-_{ij}x^-_{kl}}{x^-_{ik}x^-_{jl}} =: \chi^-_{ijkl}, \tag{2.9}$$

with $x_{ij} := x_i - x_j$. The indices in the cross-ratios $\chi^{\pm}_{ijkl}$ are labeled mod $\tilde{n}$, and the subscripts $\pm$ in $x^{\pm}_{ij}$ are space-time indices, not to be confused with the shift of θ.

It follows from (2.2) and (2.6) that the Y-functions satisfy the following Y-system

$$Y^+_j Y^-_j = (1 + Y_{j-1})(1 + Y_{j+1})\,, \tag{2.10}$$

where $j = 1, \ldots, \tilde{n}-3$. These are the main equations that characterize the present Y-functions. In addition, the Y-functions for minimal surfaces in AdS_3 obey additional conditions. One is

$$\overline{Y_j(\theta)} = Y_j(-\bar{\theta}), \tag{2.11}$$

which follows from the reality condition of the minimal surfaces. Another important condition is the asymptotic behavior for small spectral parameter $\zeta = e^{\theta} \to 0$,

$$\log Y_{2k} \sim \frac{Z_{2k}}{\zeta}\,, \quad \log Y_{2k+1} \sim \frac{Z_{2k+1}}{i\zeta}\,, \tag{2.12}$$

with moduli parameters Z_j. This behavior is determined as follows: For large $|z|$, the small solutions behave as $s_j \sim \exp(w/\zeta + \bar{w}\zeta)$, where $w = \int^z \sqrt{p(z)}dz$ with

$p(z)$ being the $(\tilde{n}-2)$-th degree polynomial associated with the minimal surface [6]. By the WKB analysis one finds that the Y-functions behave as in (2.12) with $Z_j = -\oint_{\gamma_j}\sqrt{p(z)}dz$. Namely, Z_j are period integrals over cycles γ_j of the Riemann surface $y^2 = p(z)$. γ_j are taken in such a way that each of them has nonzero intersection with the adjacent ones $\gamma_{2k}\wedge\gamma_{2k-1} = \gamma_{2k}\wedge\gamma_{2k+1} = 1$ [8]. For later convenience, we rewrite Z_j as "mass" parameters

$$m_{2k} = -2Z_{2k}\,, \quad m_{2k+1} = -2Z_{2k+1}/i\,. \tag{2.13}$$

The mass parameters are in general complex:

$$m_j = |m_j|e^{i\varphi_j}\,. \tag{2.14}$$

The other condition is the analyticity that the shifted Y-functions

$$\tilde{Y}_j(\theta) := Y_j(\theta + i\varphi_j) \tag{2.15}$$

are regular inside the strip

$$-\frac{\pi}{2} < \mathrm{Im}\,\theta < \frac{\pi}{2}. \tag{2.16}$$

Incorporating these additional conditions, one can transform the Y-system relations (2.10) into the following TBA type integral equations

$$\log\tilde{Y}_j(\theta) = -|m_j|\cosh\theta + K_{j,j-1} * \log(1+\tilde{Y}_{j-1}) + K_{j,j+1} * \log(1+\tilde{Y}_{j+1}) \tag{2.17}$$

for $|\varphi_j - \varphi_{j\pm1}| < \pi/2$, where

$$K_{jj'}(\theta) := \frac{1}{2\pi}\frac{1}{\cosh(\theta + i\varphi_j - i\varphi_{j'})} \tag{2.18}$$

and $f * g := \int f(\theta-\theta')g(\theta')d\theta'$. The free energy associated with the TBA system is expressed by the solutions of the above TBA equations as

$$-F = A_{\mathrm{free}} = \sum_{j=1}^{\tilde{n}-3}\int_{-\infty}^{\infty}\frac{d\theta}{2\pi}|m_j|\cosh\theta\log\bigl(1+\tilde{Y}_j(\theta)\bigr). \tag{2.19}$$

This gives the main contribution to the area of the minimal surfaces.

2.3. Remainder function

The TBA equations (2.17) completely determine the Y-functions. The area of the minimal surface and the reminder function are then computed by using these Y-functions. The remainder function is defined as

$$R = A - A_{\rm div} - A_{\rm BDS}, \tag{2.20}$$

where A is the area of the minimal surface, $A_{\rm div}$ and $A_{\rm BDS}$ are respectively the divergent term and the finite term read from the BDS conjecture [6]. The formulas for the $2\tilde{n}$-point amplitudes are different for odd $\tilde{n}$ and even $\tilde{n}$. We describe them separately below.

2.3.1. Case with odd $\tilde{n}$

In this case, the remainder function reads

$$R = A_{\rm sinh} + A_{\rm periods} + \Delta A_{\rm BDS}\,. \tag{2.21}$$

The first term is

$$A_{\rm sinh} = A_{\rm free} + (\tilde{n}-2)A_{\rm sinh}^{\tilde{n}=3}\,, \tag{2.22}$$

where $A_{\rm sinh}^{\tilde{n}=3} = 7\pi/12$ is the value for the hexagon solution, which necessarily becomes equivalent to the regular hexagon solution.

The second term is given by [6]

$$A_{\rm periods} = i\sum_{r=1}^{(\tilde{n}-3)/2}\left(\bar{w}_r^e w^{m,r} - w_r^e \bar{w}^{m,r}\right), \tag{2.23}$$

where $w_r^e = \oint_{\gamma_r^e}\sqrt{p(z)}dz$ and $w^{m,r} = \oint_{\gamma^{m,r}}\sqrt{p(z)}dz$ are the periods for the cycles with the canonical intersection form $\gamma_r^e \wedge \gamma^{m,s} = \delta_r^s$. In terms of the periods Z_j, which correspond to cycles with nontrivial intersection form $\theta^{jk} = \gamma_j \wedge \gamma_k$ (see [8]), it is written as

$$A_{\rm periods} = -iw_{jk}Z^j\bar{Z}^k. \tag{2.24}$$

Here, w_{jk} is the inverse of the intersection form θ^{jk}.

The third term is given by [6]

$$\Delta A_{\rm BDS} = A_{\text{BDS-like}} - A_{\rm BDS} = \frac{1}{4}\sum_{i,j=1}^{\tilde{n}}\log\frac{c_{i,j}^+}{c_{i,j+1}^+}\log\frac{c_{i-1,j}^-}{c_{i,j}^-}\,. \tag{2.25}$$

$A_{\text{BDS-like}}$ is a finite term left after subtracting A_{div} from the area of a certain reference region. $c^{\pm}_{i,j}$ are cross-ratios formed by nearest neighbor distances only. For example, when $(j-i)>0$ is odd,

$$c^{\pm}_{i,j}=\frac{x^{\pm}_{i+2,i+1}x^{\pm}_{i+4,i+3}\cdots x^{\pm}_{j,i}}{x^{\pm}_{i+1,i}x^{\pm}_{i+3,i+2}\cdots x^{\pm}_{j,j-1}}, \tag{2.26}$$

where $x_i, x_{i+1}, \ldots, x_j$ successively appear in the expression. When $(j-i)>0$ is even the path goes along the opposite side: $x_i \to x_{i-1} \to \cdots \to x_j$. By definition, $c^{\pm}_{i,j}=c^{\pm}_{j,i}$. The indices of $c^{\pm}_{i,j}$ are labeled mod $\tilde{n}$. We also define $c^{\pm}_{i,j}=1$ for $|i-j|\leq 1$. For the AdS_3 kinematics, one can set the coordinates of the cusps so that $c^{\pm}_{i,j}>0$. Note that one can express $c^{\pm}_{i,j}$ in terms of Y-functions at special values by using (2.7), (2.9).

2.3.2. Case with even $\tilde{n}$

In this case,

$$R=A_{\text{sinh}}+A_{\text{periods}}+A_{\text{extra}}+\Delta A_{\text{BDS}}\,. \tag{2.27}$$

The first term A_{sinh} is the same as in (2.22). The second term is [6]

$$A_{\text{periods}}=i\sum_{r=2}^{(\tilde{n}-2)/2}\left(\bar{w}^{e}_{r}w^{m,r}-w^{e}_{r}\bar{w}^{m,r}\right). \tag{2.28}$$

The third term is given by

$$A_{\text{extra}}=-\frac{1}{2}(w_{\text{s}}+\bar{w}_{\text{s}})\log\gamma_1^R+\frac{1}{2i}(w_{\text{s}}-\bar{w}_{\text{s}})\log\gamma_1^L\,, \tag{2.29}$$

where

$$e^{w_{\text{s}}+\bar{w}_{\text{s}}}=-\frac{x^{+}_{23}x^{+}_{45}\cdots x^{+}_{\tilde{n},1}}{x^{+}_{12}x^{+}_{34}\cdots x^{+}_{\tilde{n}-1,\tilde{n}}}\,,\quad e^{(w_{\text{s}}-\bar{w}_{\text{s}})/i}=-\frac{x^{-}_{23}x^{-}_{45}\cdots x^{-}_{\tilde{n},1}}{x^{-}_{12}x^{-}_{34}\cdots x^{-}_{\tilde{n}-1,\tilde{n}}}\,, \tag{2.30}$$

and

$$\gamma_1^L=\gamma_1(\zeta=1)\,,\quad \gamma_1^R=\gamma_1(\zeta=i)\,, \tag{2.31}$$

with

$$\gamma_1(\zeta)=T_1(\theta+\pi i)\,. \tag{2.32}$$

Here, $e^{w_{\text{s}}+\bar{w}_{\text{s}}}$, $e^{(w_{\text{s}}-\bar{w}_{\text{s}})/i}$ are given by $(T_{\tilde{n}-2})^{(-1)^{\tilde{n}/2+1}}$ at $\theta=-\pi i/2$ and 0, respectively. The relation between $\gamma_1(\zeta)$ and T_1 follows from the definition of the Stokes data. We

see that $A_{\rm extra}$ is expressed in terms of T-functions. The T-functions are expressed in terms of Y-functions, as we will see in section 4.

The last term is similar to (2.25),

$$\Delta A_{\rm BDS} = A_{\text{BDS-like}} - A_{\rm BDS} = \frac{1}{4}\sum_{i,j=1}^{\tilde{n}'} \log\frac{\hat{c}^+_{i,j}}{\hat{c}^+_{i,j+1}} \log\frac{\hat{c}^-_{i-1,j}}{\hat{c}^+_{i,j}}\,, \tag{2.33}$$

where $\tilde{n}' = \tilde{n}+1$ and $\hat{c}^\pm_{ij}$ are defined by c_{ij} for the $2(\tilde{n}+1)$-point case by the double soft limit $x^\pm_{\tilde{n}+1} \to x^\pm_1$. The explicit form is given in [22].

3. Integrable models and CFT perturbation

As we saw in the last section, the problem of computing gluon scattering amplitudes at strong coupling is governed by TBA type integral equations. It was found [9] that the above TBA equations for null-polygonal minimal surfaces in AdS_3 are identified with those of the homogeneous sine-Gordon (HSG) models [17]. In particular, when the resonance parameters are trivial, the HSG models admit the description of the bulk and boundary conformal perturbation theory (CPT). This allows us to analytically solve the TBA equations near the CFT point in the form of high-temperature (or small mass) expansion. Moreover, in some special cases the TBA equations are also identified with those of other integrable theories. In these cases, the CFT analysis becomes simpler. Furthermore, from the results for the trivial resonance parameters one is able to analyze the case of nontrivial resonance parameters, as is discussed later on. In this section we review those integrable models associated with the TBA equations and the high-temperature expansion of the free energy.

3.1. Homogeneous sine-Gordon model

The HSG models are obtained as integrable perturbations [23] of the coset $\mathrm{G}_k/\mathrm{U}(1)^{r_{\rm G}}$ CFTs (generalized parafermion CFTs) [18, 24]. Here, k is the level and $r_{\rm G}$ is the rank of a compact Lie group G. For the present purpose we focus on the case with $\mathrm{G} = \mathrm{SU}(n)$. The classical action is

$$S = k\Big(S_{\rm gWZW} - \int d^2x\, V(g)\Big)\,, \tag{3.1}$$

where $S_{\rm gWZW}$ is the corresponding gauged WZW action, g is an element of G, and

$$V(g) = \frac{\mu^2}{4\pi}\mathrm{tr}(\Lambda_+ g^\dagger \Lambda_- g)\,. \tag{3.2}$$

$\Lambda_\pm = i\boldsymbol{\lambda}_\pm \cdot \boldsymbol{h}$ are elements of the Cartan subalgebra $\mathfrak{h}$ of the Lie algebra $\mathfrak{g} = \mathfrak{su}(n)$, which are parametrized by two $(n-1)$-dimensional vectors

$$\boldsymbol{\lambda}_\pm = \sum_{i=1}^{n-1} \tilde{\mu}_i e^{\pm\sigma_i} \boldsymbol{\lambda}_i \,. \tag{3.3}$$

Here $\boldsymbol{\lambda}_i$ are the fundamental weights, the parameters σ_i describe the resonance when they are real and together with a bare overall mass scale μ, dimensionless parameters $\tilde{\mu}_i$ give the semi-classical masses of the solitons

$$\mu_i^a = \mu\tilde{\mu}_i\rho_a \,, \qquad \rho_a = \frac{\sin\frac{\pi a}{k}}{\sin\frac{\pi}{k}} \quad (a = 1, ..., k-1) \,. \tag{3.4}$$

The potential is identified with a linear combination of weight-zero adjoint fields. One can also rewrite the potential $V(g)$ as

$$V(g) = \frac{\mu^2}{4\pi} \sum_{i,j=1}^{n-1} \mu_{ij}^2 \Gamma_{ij}(g) \,, \tag{3.5}$$

with

$$\mu_{ij}^2 = \tilde{\mu}_i\tilde{\mu}_j e^{\sigma_i - \sigma_j} \,, \quad \Gamma_{ij}(g) = -\mathrm{tr}\Big((\boldsymbol{\lambda}_i \cdot \boldsymbol{h}) g^\dagger (\boldsymbol{\lambda}_j \cdot \boldsymbol{h}) g\Big) \,, \tag{3.6}$$

so that it becomes manifest that each mass scale μ_{ij} is turned on by the field Γ_{ij}.

Let us now consider the quantum theory. For the reason explained in the next subsection, we set $\sigma_i = 0$. In the quantum theory, the adjoint fields have conformal dimensions

$$\Delta = \bar{\Delta} = \frac{n}{k+n}. \tag{3.7}$$

Thus, as in the case of the sine-Gordon model [25], on dimensional grounds the potential is renormalized as

$$V \sim \sum_{i,j=1}^{n-1} (M^2 \tilde{M}_i \tilde{M}_j)^{1-(\Delta+\bar{\Delta})/2} \Big[\Gamma_{ij}(g)\Big]_{\mathcal{R}}. \tag{3.8}$$

As in the bare case, M is the physical mass scale and $\tilde{M}_i$ are dimensionless parameters, in terms of which the physical masses are expressed as

$$M_i^a = M_i \rho_a \,, \quad M_i = M\tilde{M}_i \,. \tag{3.9}$$

Replacing $\Big[\Gamma_{ij}(g)\Big]_{\mathcal{R}}$ with the weight-zero adjoint operators, the action in the quantum theory may be given by

$$S = kS_{\mathrm{gWZW}} + \lambda \int d^2x \, \Phi_{\boldsymbol{\lambda},\bar{\boldsymbol{\lambda}}} \,, \tag{3.10}$$

where

$$\begin{aligned}\Phi_{\boldsymbol{\lambda},\bar{\boldsymbol{\lambda}}} &= (\boldsymbol{\lambda})^l(\bar{\boldsymbol{\lambda}})^{\bar{l}}\phi_{l,\bar{l}} \\ &= \sum_{i,j=1}^{n-1}(\tilde{M}_i\tilde{M}_j)^{1-(\Delta+\bar{\Delta})/2}(\hat{\boldsymbol{\lambda}}_j)^l(\hat{\boldsymbol{\lambda}}_i)^{\bar{l}}\phi_{l,\bar{l}}\,. \end{aligned} \tag{3.11}$$

Here, $\phi_{l,\bar{l}}$ are the adjoint operators which transform as the l-th ($\bar{l}$-th) element of $\mathfrak{h}$ under the left (right) transformation. We have set $\sigma_i = 0$ and hence $\boldsymbol{\lambda} = \bar{\boldsymbol{\lambda}}$. One can decompose them as

$$\boldsymbol{\lambda} = \bar{\boldsymbol{\lambda}} = \sum_{j=1}^{n-1}\tilde{M}_j^{1-(\Delta+\bar{\Delta})/2}\hat{\boldsymbol{\lambda}}_j\,, \tag{3.12}$$

where each basis vector $\hat{\boldsymbol{\lambda}}_j$ corresponds to the deformation along which $\tilde{M}_j$ varies. Classically $\hat{\boldsymbol{\lambda}}_j$ coincide with the fundamental weights $\boldsymbol{\lambda}_j$, but quantum mechanically they are functions of the ratios of $\tilde{M}_j$. The coupling constant is related to the mass scale M as[1]

$$\lambda = -\kappa_n M^{2-(\Delta+\bar{\Delta})}\,. \tag{3.13}$$

The proportionality constant κ_n is computed explicitly for some simple cases, as we will see later.

We normalize the adjoint operators as

$$\left\langle \phi_{l,\bar{l}}(z)\phi_{l',\bar{l}'}(0)\right\rangle = \delta_{ll'}\delta_{\bar{l}\bar{l}'}\frac{1}{|z|^{4\Delta}}\,, \tag{3.14}$$

from which

$$\left\langle \Phi_{\boldsymbol{\lambda},\bar{\boldsymbol{\lambda}}}(z)\Phi_{\boldsymbol{\lambda},\bar{\boldsymbol{\lambda}}}(0)\right\rangle = \frac{G^2}{|z|^{\frac{4n}{n+2}}}\,, \qquad G(\tilde{M}_j) := \sum_{i,j=1}^{n-1}\tilde{M}_i^{\frac{2}{n+2}}F_{ij}\tilde{M}_j^{\frac{2}{n+2}}\,, \tag{3.15}$$

where

$$F_{ij} = \hat{\boldsymbol{\lambda}}_i\cdot\hat{\boldsymbol{\lambda}}_j. \tag{3.16}$$

Note that in the classical limit F_{ij} coincides with the inverse of the Cartan matrix.

[1]Throughout this paper, we consider the perturbation with a negative coupling constant λ.

3.2. Correspondence with minimal surfaces in AdS_3

Let us consider the SU(n) HSG model at level $k = 2$. For the case with $k = 2$, we can drop the index a in M_i^a and absorb ρ_a into M. In [26], the exact S-matrix of HSG models associated with simply laced $\mathfrak{g}$ is proposed. For the SU$(n)_2$ HSG model, the S-matrix reads [27]

$$S_{jk}(\theta) \;=\; (-1)^{\delta_{jk}}\Big[c_j \tanh\frac{1}{2}(\theta+\sigma_j-\sigma_k-\frac{\pi}{2}i)\Big]^{I_{jk}} \tag{3.17}$$

for $j, k = 1, ..., n-1$, where δ_{jk} is the Kronecker delta, $c_j = \pm 1$, and I_{jk} is the incidence matrix for $\mathfrak{su}(n)$. Given the S-matrix, one can write down the TBA equations for the HSG models [27–29] as

$$\epsilon_j(\theta) = M_j L\cosh\theta - K_{jk} * \log(1+e^{-\epsilon_k}), \tag{3.18}$$

where L denotes the inverse temperature and the kernel is given by

$$K_{jk} = i\frac{\partial}{\partial\theta}\ln S_{jk}. \tag{3.19}$$

As usual, the pseudo energies $\epsilon_j(\theta)$ are related to the Y-functions as

$$\tilde{Y}_j = e^{-\epsilon_j}. \tag{3.20}$$

It was found in [9] that the above TBA equations coincide with those for the minimal surfaces in AdS_3 (2.17) under the identification

$$n = \tilde{n} - 2, \qquad M_j L = |m_j|, \qquad \sigma_j = i\varphi_j. \tag{3.21}$$

Note that the TBA equations for the minimal surfaces with complex masses ($\varphi_j \neq 0$) correspond to those for the HSG model with purely imaginary resonance parameters. Physical interpretation of such resonance parameters in the HSG model is not quite clear at present. In addition, when $\sigma_j - \sigma_k$ are nonzero, the boundary Yang–Baxter equations [30] are not satisfied and the boundary factorizable scattering may not be well-defined. These are the reasons why we have set $\sigma_j = 0$ in the last subsection. Also, with this restriction one can make full use of the known results about the high-temperature expansion, as we see in the following. We will discuss how to incorporate σ_j in later sections.

3.3. Bulk perturbation of free energy

The free energy of the model on a space of length $R \gg 1$ with temperature $1/L$ (in the L-channel) gives the ground state energy of the model on a space of length L (in the R-channel) [12]. The free energy around the CFT point is then given by evaluating the ground state energy of the perturbed CFT on a cylinder of circumference L with small coupling constant λ. From the action (3.10), the conformal perturbation theory (CPT) gives an expansion of the free energy[2]

$$\begin{aligned} -F \;=\; A_{\rm free} \;&=\; \frac{\pi}{6}c_n + f_n^{\rm bulk} + (2\pi)^2 \sum_{k=1}^{\infty} \frac{(-\lambda)^k}{k!} \Big(\frac{2\pi}{L}\Big)^{2(\Delta-1)k} \\ &\quad \times \int \Big\langle \Phi_{\boldsymbol{\lambda},\bar{\boldsymbol{\lambda}}}(z_1,\bar{z}_1)\cdots\Phi_{\boldsymbol{\lambda},\bar{\boldsymbol{\lambda}}}(z_k,\bar{z}_k)\Big\rangle_{\rm connected} \prod_{i=2}^{k} (z_i\bar{z}_i)^{\Delta-1} dz_2^2\cdots dz_k^2 \\ &:= \frac{\pi}{6}c_n + f_n^{\rm bulk} + \sum_{k=2}^{\infty} f_n^{(k)} l^{\frac{4k}{n+2}}. \end{aligned} \tag{3.22}$$

Here, $l = ML$ denotes the scale parameter, c_n is the central charge and $f_n^{\rm bulk}$ is the bulk term. We have set $z_1 = 1$ by using translational invariance. We have used the fact that the coupling constant λ has mass dimension $2 - 2\Delta = \frac{4}{n+2}$ and is proportional to $l^{\frac{4}{n+2}}$. We have also used the fact that the one-point function vanishes. The central charge of the coset $\mathrm{SU}(n)_2/\mathrm{U}(1)^{n-1}$ is

$$c_n = \frac{n(n-1)}{n+2}. \tag{3.23}$$

The bulk term $f_n^{\rm bulk}$ may be obtained as a generalization of the results in the literature [12,31,33,34]. For odd n, following the procedure in [12,33] (see also [35]) one arrives at the expression[3]

$$f_n^{\rm bulk} = \frac{1}{4} l^2 \sum_{i,j=1}^{n-1} \tilde{M}_i (I^{-1})_{ij} \tilde{M}_j \,. \tag{3.24}$$

Note that the incidence matrix I_{ij} has the inverse for odd n. For even n, following the analysis in [34] one obtains

$$f_n^{\rm bulk} = \frac{1}{(n+2)\pi} Q^2 \cdot l^2 \log l \,, \tag{3.25}$$

[2]We have rescaled the free energy as $L^2F/R \to F$.

[3]In the course of the derivation in the references, Δ is assumed to be sufficiently small, so that the terms in the summation in (3.22) are smaller than l^2. As this condition is not valid in our case with $\Delta = n/(n+2)$, one needs appropriate modification for a rigorous derivation. We have checked for $n = 3$ that the expression (3.24) is in good agreement with numerical results.

where

$$Q := \sum_{j=0}^{n/2-1} (-)^j \tilde{M}_{2j+1} \,. \tag{3.26}$$

(3.24)–(3.26) reproduce the known results in the case of a single nonzero mass [31, 34, 36].

The coefficients $f_n^{(k)}$ are obtained by computing CFT correlation functions. Since we already know the two-point function, we find the lowest correction from CPT:

$$f_n^{(2)} = \frac{\pi}{6}\kappa_n^2 G^2 C_n^{(2)} \,, \quad C_n^{(2)} = 3(2\pi)^{\frac{2(n-2)}{n+2}} \gamma^2\Big(\frac{n}{n+2}\Big)\gamma\Big(\frac{2-n}{n+2}\Big) \,. \tag{3.27}$$

Here, G is given in (3.15) and we have used

$$\int d^2z\, |z|^{2a}|1-z|^{2b} = \pi\gamma(1+a)\gamma(1+b)\gamma(-1-a-b) \,. \tag{3.28}$$

In section 6, we present the explicit expression in the case of $n = 3$ as an illustration.

3.4. Single mass cases

The TBA equations (3.18) contain $n-1$ mass parameters. When some of them are set to be zero, the corresponding massless pseudo energies $\epsilon_j(\theta)$ become finite constants for $L \to \infty$, while massive ones become infinite [31]. This gives rise to the appearance of CFT with a different central charge. Nevertheless, one finds little difference concerning the small mass expansion: When one turns on/off some of the masses, only the constant term changes discontinuously and the other expansion coefficients changes continuously. This can be checked numerically.

For HSG models with general masses, the precise form of the perturbing operator (3.11), as a function of masses, has not yet been well understood. On the other hand, when only one mass parameter is nonzero, the CFT in the small mass limit becomes simple and the perturbing operator as well as the exact coupling–mass ratio is known. This allows us to explicitly compute the expansion coefficients at low orders. Below we present a list of such cases and collect useful facts in performing the small mass expansion.[4] Remarkably, combining the cases in subsections 3.4.1 and 3.4.3, we are able to analyze a case of two general masses, which we will discuss in section 6.

[4]The reader is referred to [37] for a more extensive classification of conformal perturbations associated with TBA equations.

3.4.1. Integrable perturbation of unitary minimal model

Let us first consider the case

$$M_1 = M, \quad \text{others} = 0. \tag{3.29}$$

The TBA equations (3.18) in this case are identified with those of the $(\mathrm{RSOS})_n$ scattering theory [31, 32]. The $(\mathrm{RSOS})_n$ scattering theory is regarded as the massive perturbation of unitary minimal model $\mathcal{M}_{n+1,n+2}$ by the primary field $\Phi_{1,3}$ with dimension $\Delta = \bar{\Delta} = \frac{n}{n+2}$. The action for the $(\mathrm{RSOS})_n$ scattering theory is

$$S_{(\mathrm{RSOS})_n} = S_{\mathcal{M}_{n+1,n+2}} + \lambda_{\mathrm{RSOS}} \int d^2x \, \Phi_{1,3} \,, \tag{3.30}$$

where the relevant operator is normalized as

$$\Big\langle \Phi_{1,3}(z)\Phi_{1,3}(0) \Big\rangle = \frac{1}{|z|^{4\Delta}} \,, \tag{3.31}$$

and the coupling λ_{RSOS} is related to the mass M_1 as [25]

$$\lambda_{\mathrm{RSOS}} = -\kappa_n^{\mathrm{RSOS}} M_1^{2(1-\Delta)} \,, \tag{3.32}$$

with

$$\kappa_n^{\mathrm{RSOS}} = \frac{1}{\pi} \frac{(n+2)^2}{n(2n+1)} \left[\gamma\Big(\frac{3(n+1)}{n+2}\Big) \gamma\Big(\frac{n+1}{n+2}\Big) \right]^{\frac{1}{2}} \left[\frac{\sqrt{\pi}\Gamma(\frac{n+2}{2})}{2\Gamma(\frac{n+1}{2})} \right]^{\frac{4}{n+2}} \,, \tag{3.33}$$

and $\gamma(x) = \Gamma(x)/\Gamma(1-x)$.

Taking into account the normalizations (3.15), (3.31), one finds that

$$\lambda G(\tilde{M}_i)\Big|_{\tilde{M}_i = 0 (i \neq 1)} = \lambda_{\mathrm{RSOS}} \,, \tag{3.34}$$

and hence

$$\lambda = -\kappa_n M^{\frac{4}{n+2}}, \qquad \kappa_n = \frac{\kappa_n^{\mathrm{RSOS}}}{F_{11}}. \tag{3.35}$$

3.4.2. Integrable perturbation of unitary SU(2) diagonal coset

The above case is generalized to the cases

$$M_k = M, \quad \text{others} = 0, \quad \text{for} \quad k = 1, \ldots, n-1. \tag{3.36}$$

It is known that the TBA equations (3.18) in these cases describe the system obtained as integrable perturbation of $(\mathrm{SU}(2)_k \times \mathrm{SU}(2)_{n-k})/\mathrm{SU}(2)_n$ coset CFT [36, 37]. The perturbing operator is the primary field $\phi_{1,1,3}$, which corresponds to the branching of the product of two trivial representations into the adjoint representation. This operator has conformal dimension $\Delta = \bar{\Delta} = \frac{n}{n+2}$. The exact coupling–mass ratio in these cases is found in [38].

3.4.3. Integrable perturbation of non-unitary SU(2) diagonal coset

Let us next consider the cases where

$$M_k = M_{n-k} = M, \quad \text{others} = 0, \quad (k = 1, \ldots, n-1) \tag{3.37}$$

with n being odd. This kind of configuration is invariant under the $\mathbb{Z}_2$ outer automorphism of the A_{n-1} Dynkin diagram. In this case, one can regard the TBA equations as those corresponding to the tadpole diagram $T_{(n-1)/2}\,(= A_{n-1}/\mathbb{Z}_2)$ with a single mass parameter being turned on. It is known that they describe the system obtained as integrable perturbation of non-unitary $(\mathrm{SU}(2)_k \times \mathrm{SU}(2)_{n/2-k-1})/\mathrm{SU}(2)_{n/2-1}$ coset CFT [37]. The perturbing operator is $\phi_{1,1,3}$ with dimension $\Delta = \bar{\Delta} = \frac{n-2}{n+2}$.

In particular, the case with $k = 1$, namely

$$M_1 = M_{n-1} = M, \quad \text{others} = 0 \tag{3.38}$$

corresponds to integrable perturbation of the non-unitary minimal models $\mathcal{M}_{n,n+2}$. The case with $n = 3$ and $k = 1$ will be used in the analysis for the decagon in section 6.

4. Conformal perturbation of *g*- and T-functions

As we saw in the previous section, the relation between the free energy in the L-channel and the ground state energy in the R-channel allows one to derive an expansion of the free energy near the CFT limit. Such an expansion is studied for the 6-point amplitudes with the AdS_5 kinematics in [13]. To obtain the full expression of the amplitudes, one further needs the expansion of the cross-ratios or the Y-/T-functions. A key observation [39, 40] for this purpose is the relationship between the T-functions and the g-functions [14]. In this section, we discuss the conformal perturbation of the T-functions of the HSG model associated with the coset $\mathrm{SU}(n)_2/\mathrm{U}(1)^{n-1}$. We follow [15,40] where the perturbation of the g- and T-functions in the ADET purely elastic scattering theories is discussed. The discussion below holds for general n with trivial formal monodromy (i.e., $T_n = 1$) and will be applied to concrete examples in the following sections.[5]

4.1. *g*-functions in homogeneous sine-Gordon model

We start by considering the partition function $Z_{\langle\alpha|\alpha\rangle}[L, R]$ on a cylinder of circumference L, length R, and boundary conditions of type α at both ends. It is expanded

[5]For even n, one can consider the cases with non-trivial T_n, where the discussion may need some modifications. Such cases appear for $2n + 4 \geq 12$, which we hope to discuss elsewhere.

by the eigenvalues of the circle Hamiltonian $H^{\rm circ}(M,L)$ as

$$Z_{\langle\alpha|\alpha\rangle}[L,R] = \langle\alpha|\, e^{-RH^{\rm circ}(M,L)}|\alpha\rangle = \sum_{p=0}^{\infty}\Big(\mathcal{G}^{(p)}_{|\alpha\rangle}(l)\Big)^2 e^{-RE_p^{\rm circ}(M,L)}\,, \tag{4.1}$$

where M is the mass scale defined through $M_k = \tilde{M}_k M$,

$$\mathcal{G}^{(p)}_{|\alpha\rangle}(l) = \frac{\langle\alpha|\psi_p\rangle}{\langle\psi_p|\psi_p\rangle^{1/2}} \tag{4.2}$$

with $|\psi_p\rangle$ being the eigenstates of the Hamiltonian, and $l = ML$. The g-function is then defined by subtracting the linear term in L from $\mathcal{G}^{(0)}_{|\alpha\rangle}(l)$:

$$\log g_{|\alpha\rangle}(l) = \log \mathcal{G}^{(0)}_{|\alpha\rangle}(l) + f_{|\alpha\rangle}L\,. \tag{4.3}$$

$f_{|\alpha\rangle}$ is the constant boundary contribution to the ground state energy $E_0^{\rm strip}$ of the L-channel Hamiltonian $H^{\rm strip}_{\langle\alpha|\alpha\rangle}(R)$. The g-function counts the ground state degeneracy and is known to decrease along the renormalization flow [14]. It is also a subleading contribution to the partition function for large R.

To consider the g-functions in the HSG model, we assume that the HSG model admits an integrable generalization with boundaries, and the boundary scattering amplitudes are also diagonal. In this section, we also set the parity breaking parameters $\sigma_j = 0$ as discussed in section 3. We will discuss how to incorporate σ_j in later sections.

In the presence of boundaries, one has the boundary reflection factors $R_j(\theta)$, which are constrained by unitarity and crossing-unitarity [41, 42],

$$R_j(\theta)R_j(-\theta) = 1\,, \quad R_j(\theta)R_{\bar{\jmath}}(\theta - i\pi) = S_{jj}(2\theta)\,, \tag{4.4}$$

where the anti-particles are the same as the particles in our case, $\bar{\jmath} = j$. The boundary Yang-Baxter equations are indeed satisfied for $\sigma_{jk} := \sigma_j - \sigma_k = 0$. In general, reflection factors also have to satisfy the boundary bootstrap equations. They are, however, trivial in our case, since the bulk S-matrix (3.17) with $\sigma_{jk} = 0$ does not have poles in the physical strip $0 \le \mathrm{Im}\,\theta \le \pi$. The form of the constraints (4.4) shows that a set of reflection factors $R_j(\theta)$ generates another $R'_j = R_j/Z_j$, if $Z_j(\theta)$ are a solution to one-index versions of the bulk unitary and crossing-unitary equations [43],

$$Z_j(\theta)Z_j(-\theta) = 1\,, \quad Z_j(\theta)Z_{\bar{\jmath}}(\theta - i\pi) = 1\,. \tag{4.5}$$

In particular, we use a solution,

$$Z_j^{|k,C\rangle}(\theta) := \Big((1+C)_\theta(1-C)_\theta\Big)^{\delta_{jk}}, \tag{4.6}$$

in the following, where

$$(x)_\theta := \frac{\sinh\frac{1}{2}(\theta + i\frac{\pi}{2}x)}{\sinh\frac{1}{2}(\theta - i\frac{\pi}{2}x)}\,. \tag{4.7}$$

A boundary α is then associated with a set of the reflection factors $R_j^{|\alpha\rangle}(\theta)$. It turns out that the g-function corresponding to $|\alpha\rangle$ satisfies the following integral equation [15, 16, 44, 45],

$$\begin{aligned}\log g_{|\alpha\rangle}(l) \;=\; &\log C_{|\alpha\rangle} + \Sigma(l) \\ &+ \frac{1}{4}\sum_{j=1}^{n-1}\int_{\mathbb{R}} d\theta \left(\phi_j^{|\alpha\rangle}(\theta) - \delta(\theta) - 2\phi_{jj}(2\theta)\right)\log\left(1 + e^{-\epsilon_j(\theta)}\right)\,.\end{aligned} \tag{4.8}$$

Here, $C_{|\alpha\rangle}$ is a symmetry factor associated with the vacuum degeneracy at infinite l. $\phi_j^{|\alpha\rangle}$ and ϕ_{jk} are given by the boundary and bulk S-matrices as

$$\phi_j^{|\alpha\rangle}(\theta) = \frac{1}{\pi i}\partial_\theta \log R_j^{|\alpha\rangle}(\theta)\,, \quad \phi_{jk}(\theta) = \frac{1}{2\pi i}\partial_\theta \log S_{jk}(\theta)\,. \tag{4.9}$$

$\Sigma(l)$ is a certain boundary-condition independent term, precise form of which is irrelevant for our purpose. For details, see [15, 16].

4.2. Relation between g- and T-functions

In the conformal limit, boundary conditions are labeled by primary fields, and hence a boundary α may be specified by the corresponding primary field. To describe the relation between the g- and the T-functions, we then consider the reflection factors corresponding to the boundary condition labeled by the identity operator, $R_j^{|\mathbb{1}\rangle}(\theta)$, together with the deformed ones,

$$R_j^{|k,C\rangle}(\theta) = \frac{R_j^{|\mathbb{1}\rangle}(\theta)}{Z_j^{|k,C\rangle}(\theta)}\,. \tag{4.10}$$

$R_j^{|\mathbb{1}\rangle}$ is expected to be minimal, namely, having the smallest number of poles and zeros. We assume the existence of $R_j^{|\mathbb{1}\rangle}$. These reflection factors give the g-functions $g_{|\mathbb{1}\rangle}$ and $g_{|k,C\rangle}$ through (4.8), the ratio of which satisfies an integral equation,

$$\begin{aligned}&\log\left(\frac{g_{|k,C\rangle}(l)}{g_{|\mathbb{1}\rangle}(l)}\frac{C_{|\mathbb{1}\rangle}}{C_{|k,C\rangle}}\right) \\ &\qquad = \int\frac{d\theta}{4\pi}\left(\frac{1}{\cosh(\theta + i\frac{\pi}{2}C)} + \frac{1}{\cosh(\theta - i\frac{\pi}{2}C)}\right)\log\Big(1 + Y_k(\theta)\Big)\,.\end{aligned} \tag{4.11}$$

We notice that almost only the information of the deforming factors $Z_j^{|k,C\rangle}$ has remained.

On the other hand, from the T-system (2.2) and the relation between the T- and Y-functions (2.6), the T-functions obey the integral equation, [6]

$$\log T_k(\theta) = -\nu_k \cosh\theta + K * \log(1+Y_k)\,. \tag{4.12}$$

Here, the kernel is given by (2.18) with $\varphi_j = \varphi_{j'} = 0$: $K = 1/(2\pi\cosh\theta)$. ν_k specify the asymptotic behavior of $T_k(\theta)$ and are related to the mass term of the TBA equations as

$$m_k = \nu_{k-1} + \nu_{k+1}\,. \tag{4.13}$$

Comparing (4.11) and (4.12), and using $T_k(\theta) = T_k(-\theta)$, one finds that

$$\log\left(\frac{g_{|k,C\rangle}(l)}{g_{|\mathbb{1}\rangle}(l)}\frac{C_{|\mathbb{1}\rangle}}{C_{|k,C\rangle}}\right) = \nu_k \cos\Big(\frac{\pi}{2}C\Big) + \log T_k\Big(i\frac{\pi}{2}C\Big)\,. \tag{4.14}$$

Since $C_{|\alpha\rangle}$ is associated with the vacuum degeneracy, which may be determined by the symmetry, we expect $C_{|\mathbb{1}\rangle} = C_{|k,C\rangle}$. Assuming this and subtracting the linear term in $l \propto \nu_k$, we arrive at an important formula,

$$\frac{\mathcal{G}^{(0)}_{|k,C\rangle}}{\mathcal{G}^{(0)}_{|\mathbb{1}\rangle}} = T_k\Big(i\frac{\pi}{2}C\Big)\,. \tag{4.15}$$

4.3. Expansion of T-functions

Using (4.15) and the conformal perturbation, one can derive an expansion of $T_k(\theta)$ near the CFT limit. To this end, we first note that the conformal perturbation gives the expansion of the g-functions [15, 40],

$$\begin{aligned}
\log \mathcal{G}^{(0)}_{|\mathbb{1}\rangle}(\lambda, L) &= \sum_{q=0}^{\infty} g_q^{|\mathbb{1}\rangle}(\lambda L^{2-2\Delta})^q\,, \\
\log \mathcal{G}^{(0)}_{|\alpha\rangle}(\lambda, \mu, L) &= \sum_{p,q=0}^{\infty} g_{p,q}^{|\alpha\rangle}(\mu L^{1-\Delta})^p(\lambda L^{2-2\Delta})^q\,,
\end{aligned} \tag{4.16}$$

where μ is the coupling of the boundary perturbation, and we have assumed that the dimension of the boundary perturbing operator is $\Delta = n/(n+2)$. Following the

[6] For even n, an appropriate gauge has to be chosen.

argument in [15], we also assume the relation between the boundary coupling and the deformation parameter,

$$\mu = \mu_0 \cos\Big(\frac{\pi}{n+2}C\Big)\,, \tag{4.17}$$

where μ_0 is some constant. Together with (4.15), this relates the boundary coupling μ to the argument of $T_k(\theta)$. (4.17) also means that the boundary coupling vanishes at $C = (n+2)/2$. In this case, the boundary conditions become conformal and are described by (linear combinations of) the Cardy boundary states. The conformal perturbation with only the bulk coupling λ turned on then gives [15, 40]

$$\log \mathcal{G}_{|\alpha\rangle}(\lambda, L) := \log\langle\alpha|\Omega\rangle = \log g_{|\alpha\rangle} + \lambda d_1^{|\alpha\rangle} L^{2(1-\Delta)} + \cdots. \tag{4.18}$$

Here, $|\Omega\rangle$ is the full ground state,

$$d_1^{|\alpha\rangle} = -\frac{1}{2(2\pi)^{1-2\Delta}} \frac{g^{\Phi}_{|\alpha\rangle}}{g_{|\alpha\rangle}} B(1-2\Delta, \Delta)\,, \tag{4.19}$$

and $B(a,b) = \Gamma(a)\Gamma(b)/\Gamma(a+b)$ is the Euler beta function. We have also introduced

$$g_{|\alpha\rangle} := \langle\alpha|0\rangle\,, \quad g^{\Phi}_{|\alpha\rangle} := \langle\alpha|\Phi\rangle\,, \tag{4.20}$$

with $|0\rangle$ and $|\Phi\rangle$ being the CFT vacuum state and the state corresponding to the bulk perturbing field $\Phi = \Phi_{\boldsymbol{\lambda},\bar{\boldsymbol{\lambda}}}$, respectively. $\mathcal{G}_{|\alpha\rangle}$ is different from $\mathcal{G}^{(0)}_{|\alpha\rangle}$ in (4.2) by a normalization factor $\langle\Omega|\Omega\rangle^{1/2}$, but this factor is cancelled in the formula (4.15).

On the T-function side, we first note that the Y-functions for the $2(n+2)$-point amplitudes have the periodicity,

$$Y_k\Big(\theta + i\pi\frac{n+2}{2}\Big) = Y_{n-k}(\theta)\,. \tag{4.21}$$

Y_k are also analytic for finite θ, and even functions of θ, $Y_k(\theta) = Y_k(-\theta)$. These properties are common to the T-functions, which leads to the expansion [11],

$$T_k(\theta) \;=\; \sum_{p=0}^{\infty} c_k^{(p)}(l) \cosh\Big(\frac{2p}{n+2}\theta\Big)\,, \tag{4.22}$$

with

$$c_k^{(2q)}(l) = c_{n-k}^{(2q)}(l)\,, \quad c_k^{(2q+1)}(l) = -c_{n-k}^{(2q+1)}(l) \quad (q \in \mathbb{Z}_{\geq 0})\,. \tag{4.23}$$

For small l, the coefficients behave as $c_k^{(p)}(l) \sim l^{(1-\Delta)p}$, since the Y- and T-functions show plateaus for $-\log(1/l) \ll \theta \ll \log(1/l)$. The conformal perturbation (4.16) further suggests that $c_k^{(p)}(l)$ are expanded as

$$c_k^{(p)}(l) = \sum_{q=0}^{\infty} c_k^{(p,2q)} l^{(1-\Delta)(p+2q)}\,. \tag{4.24}$$

(See Appendix C and D for details.) The Y-functions have a similar expansion. Similar double expansions have been discussed also for other TBA systems [13, 46]. Substituting this expansion into the Y-system (2.10), one then finds that some lower coefficients vanish. In term of the T-functions, the result reads

$$c_k^{(0)}(l) = c_k^{(0,0)} + o\big(l^{3(1-\Delta)}\big)\,, \quad c_k^{(1)}(l) = 0 + o\big(l^{3(1-\Delta)}\big)\,,$$
$$c_k^{(2)}(l) = c_k^{(2,0)} l^{2(1-\Delta)} + o\big(l^{3(1-\Delta)}\big)\,. \tag{4.25}$$

Now, from (4.15), (4.18), (4.22) and (4.25) with $C = (n+2)/2$, the expansion of $T_k(\theta)$ is determined. Comparing both sides of (4.15), one first notices that the two expansions (4.16) and (4.25) are consistent with each other, once $g_{1,0}^{|\alpha\rangle} = 0$ is taken into account, meaning that the one-point functions of the boundary perturbing operator vanish in unitary theories. Furthermore,

$$T_k(\theta) = c_k^{(0,0)} + c_k^{(2,0)} l^{2(1-\Delta)} \cosh\Big(\frac{4\theta}{n+2}\Big) + \mathcal{O}(l^{3(1-\Delta)})\,, \tag{4.26}$$

where

$$c_k^{(0,0)} = \frac{g_{|k\rangle}}{g_{|\mathbb{1}\rangle}}\,, \quad c_k^{(2,0)} = \frac{g_{|k\rangle}}{g_{|\mathbb{1}\rangle}}\big(d_1^{|k\rangle} - d_1^{|\mathbb{1}\rangle}\big)\kappa_n\,, \tag{4.27}$$

and we have used (3.13). We have also set $g_{|k,C\rangle} =: g_{|k\rangle}$, $g^{\Phi}_{|k,C\rangle} =: g^{\Phi}_{|k\rangle}$ and $d_1^{|k,C\rangle} =: d_1^{|k\rangle}$, since they are evaluated for the unperturbed boundary states which are independent of μ and hence of C.

In the course of deriving the above formula, we have made several assumptions following [15, 40]: the existence of integrable boundary perturbations of the HSG model by operators with dimension Δ, that of the reflection factors associated with the identity operator, the invariance of the symmetry factor $C_{|\mathbb{1}\rangle}$ under the deformation, and the relation (4.17). We will check that these are consistent with numerical computations and the results in the conformal limit, which we discuss shortly.

4.4. Identification of boundary conditions

When evaluating the expansion (4.26), we need to identify the boundary conditions represented by the reflection factors (4.10). For this purpose, we first recall that the Cardy boundary states are of the form

$$|\alpha\rangle = \sum_{\rho} \frac{S_{\alpha\rho}}{\sqrt{S_{0\rho}}} |\rho\rangle\!\rangle\,, \tag{4.28}$$

where $|\rho\rangle\!\rangle$ are the Ishibashi states. In our case of the $\mathrm{SU}(n)_2/\mathrm{U}(1)^{n-1}$ coset CFT, the modular S-matrix, $S_{\rho\rho'}$, is given by the product of the S-matrix for $\mathrm{SU}(n)_2$ and the complex conjugate of the S-matrix for $\mathrm{U}(1)^{n-1}$: $S_{\rho\rho'} = S^{(2)}_{\boldsymbol{\rho}\boldsymbol{\rho}'} S^*_{\mathfrak{u}(1)}$. Here, $\boldsymbol{\rho} := [\rho_1, ..., \rho_{n-1}]$ is the Dynkin label of $\mathfrak{su}(n)$. Since we deal only with primaries whose $\mathfrak{u}(1)$ weights are zero, the $\mathfrak{u}(1)$ part is trivial and hence we drop $S^*_{\mathfrak{u}(1)}$ in the following.

In general, the index of the T-functions labels the representations of the underlying symmetry. Thus, we infer that $R_j^{|k,C\rangle}$ correspond to the k-th fundamental representation with the Dynkin label whose components are $(\boldsymbol{\rho}_k)_j = \delta_{j,k}$. It then follows that

$$g_{|\mathbb{1}\rangle} = \frac{S^{(2)}_{\mathbf{00}}}{\sqrt{S^{(2)}_{\mathbf{00}}}}\,, \quad g_{|k\rangle} = \frac{S^{(2)}_{\boldsymbol{\rho}_k\mathbf{0}}}{\sqrt{S^{(2)}_{\mathbf{00}}}}\,. \tag{4.29}$$

Here, the S-matrix for $\mathrm{SU}(n)_2$ is given by the formula [47],

$$\begin{aligned} S^{(2)}_{\boldsymbol{\rho}\boldsymbol{\mu}} \;=\; & (n+2)^{-(n-1)/2} \frac{i^{n(n-1)/2}}{\sqrt{n}} \exp\left[\frac{2\pi i}{n(n+2)} \left(\sum_{j=1}^{n-1} j(\rho_j+1)\right)\left(\sum_{j=1}^{n-1} j(\mu_j+1)\right)\right], \\ & \times \det\left(\exp\left[-\frac{2\pi i}{n+2}\left(\sum_{j=a}^{n-1}(\rho_j+1)\right)\left(\sum_{j=b}^{n-1}(\mu_j+1)\right)\right]\right)_{1\le a,b\le n}. \end{aligned} \tag{4.30}$$

From (4.29) and (4.30), we find the CFT limit of the T- and Y-functions:

$$\begin{aligned} T_k \;&\to\; c_k^{(0,0)} = \frac{S^{(2)}_{\boldsymbol{\rho}_k\mathbf{0}}}{S^{(2)}_{\mathbf{00}}} = \frac{\sin\frac{(k+1)\pi}{n+2}}{\sin\frac{\pi}{n+2}}\,, \\ Y_k \;&\to\; \frac{S^{(2)}_{\boldsymbol{\rho}_{k-1}\mathbf{0}} S^{(2)}_{\boldsymbol{\rho}_{k+1}\mathbf{0}}}{\left(S^{(2)}_{\mathbf{00}}\right)^2} = \frac{\sin\frac{k\pi}{n+2}\sin\frac{(k+2)\pi}{n+2}}{\sin^2\frac{\pi}{n+2}}\,. \end{aligned} \tag{4.31}$$

These agree with the result in [8], which supports our formula (4.26) and identification of the boundary conditions. We note that the relation between the g-functions and the T-functions at the CFT point naturally explains the fact that the quantum dimensions (ratios of the modular S-matrices) are the solutions of the constant T-system, called the Q-system [10, 48, 49]. From the relation between the T- and g-functions, this may hold for general TBA systems.

Since the bulk perturbing operator Φ is a linear combination of the adjoint operators, $g^{\Phi}_{|\alpha\rangle}$ are similarly expressed by the elements of the modular S-matrix with the Dynkin label of the adjoint representation $\boldsymbol{\rho}_{\mathrm{adj}}$:

$$g^{\Phi}_{|\mathbb{1}\rangle} = G(\tilde{M}_i)\frac{S^{(2)}_{\mathbf{0}\boldsymbol{\rho}_{\mathrm{adj}}}}{\sqrt{S^{(2)}_{\mathbf{0}\boldsymbol{\rho}_{\mathrm{adj}}}}}\,, \quad g^{\Phi}_{|k\rangle} = G(\tilde{M}_i)\frac{S^{(2)}_{\boldsymbol{\rho}_k\boldsymbol{\rho}_{\mathrm{adj}}}}{\sqrt{S^{(2)}_{\mathbf{0}\boldsymbol{\rho}_{\mathrm{adj}}}}}\,. \tag{4.32}$$

Thus, at the leading order, both of the expansions of the free energy and the Y-functions are given in terms of $G(\tilde{M}_j)$. In addition, in order to obtain the full expressions of the scattering amplitudes, we need the explicit form of Φ, as well as the bulk coupling λ, in terms of the TBA masses m_k. These are discussed in section 6.

5. Remainder function for the octagon

As we have seen in section 2, the minimal surface with a null polygonal boundary in the AdS space is described by the Y-system or the TBA equations. The Y-functions and the T-functions play important roles in this picture. In the previous two sections, we have seen the relation between the g-functions and the T-functions in the underlying integrable model. This relation enables us to compute the high-temperature (small mass) expansions of the T-functions by using the conformal perturbation technique. Consequently, the remainder function is expanded around the kinematic configurations associated with regular polygons. Here we consider the first non-trivial example in AdS_3: the octagon. In this case, the exact expression of the remainder function at strong coupling has been computed by Alday and Maldacena [6], and one can learn much about the expansions of the T-functions and the g-functions. The underlying integrable model corresponding to the octagon is the off-critical Ising model (with a complex mass). The exact g-function for the off-critical Ising model was obtained in [16, 50, 51]. Though the TBA system of the off-critical Ising model is trivial, the high-temperature expansions of the free energy and of the T-function are still non-trivial.

As in (2.27), the remainder function is divided into several pieces:

$$R_8 = \frac{7\pi}{6} + A_{\text{free}} + A_{\text{periods}} + A_{\text{extra}} + \Delta A_{\text{BDS}}. \tag{5.1}$$

These terms are given by

$$A_{\text{free}} = \int_{-\infty}^{\infty} \frac{dt}{2\pi} l \cosh t \log\left(1 + e^{-l\cosh t}\right), \tag{5.2}$$

$$A_{\text{periods}} = 0, \tag{5.3}$$

$$A_{\text{extra}} = -\frac{l}{2}(\cos\phi \log \gamma_1^{\text{L}} + \sin\phi \log \gamma_1^{\text{R}}), \tag{5.4}$$

$$\Delta A_{\text{BDS}} = A_{\text{BDS-like}} - A_{\text{BDS}} = -\frac{1}{2}\log(1+\chi^-)\log\left(1 + \frac{1}{\chi^+}\right), \tag{5.5}$$

where

$$\chi^+ = e^{l\sin\phi}, \qquad \chi^- = e^{-l\cos\phi}, \tag{5.6}$$

and $\gamma_1^{\rm L}, \gamma_1^{\rm R}$ are obtained from (2.31) with

$$\log \gamma_1(\zeta = e^{\theta}) = \frac{1}{2\pi} \int_{-\infty}^{\infty} \frac{dt}{\cosh(t - \theta + i\phi)} \log\left(1 + e^{-l\cosh t}\right). \tag{5.7}$$

We note that (5.7) is a special case of (4.12) for $k = 1$ with $\nu_1 = 0$ and $Y_1(\theta) = e^{-l\cosh\theta}$, in accord with (2.32). Our goal here is to expand the remainder function around $l = 0$. For the octagon, we can get the all-order expansion at arbitrary ϕ.

The expansion of the free energy was studied in [33], and the result is the following,

$$\begin{aligned} A_{\rm free} = \frac{\pi}{12} - \frac{l^2}{4\pi}\left(\log\frac{1}{l} + \frac{1}{2} + \log\pi - \gamma_{\rm E}\right) \\ + \pi \sum_{k=1}^{\infty} \binom{\frac{1}{2}}{k+1} \left(1 - \frac{1}{2^{2k+1}}\right) \zeta(2k+1) \left(\frac{l}{\pi}\right)^{2k+2}, \end{aligned} \tag{5.8}$$

where $\gamma_{\rm E}$ is the Euler constant.

In order to expand $A_{\rm extra}$, we introduce the following function,

$$F(l,\varphi) = \frac{1}{2\pi} \int_{-\infty}^{\infty} \frac{dt}{\cosh(t + i\varphi)} \log(1 + e^{-l\cosh t}) \qquad \left(|\varphi| < \frac{\pi}{2}\right), \tag{5.9}$$

where $\gamma_1^{\rm L}$ and $\gamma_1^{\rm R}$ are related to this function as

$$\log \gamma_1^{\rm L} = F(l,\phi), \qquad \log \gamma_1^{\rm R} = F\left(l, \phi - \frac{\pi}{2}\right). \tag{5.10}$$

Note that this function is related to the exact g-function for the off-critical Ising model considered in [16]. In [16], the exact g-function was discussed in two special cases, which essentially reduce to $\varphi = 0$ in our case. $\varphi \neq 0$ corresponds to the case that the boundary magnetic field is turned on in the off-critical Ising model. Here we obtain the small l expansion of the g-function for general values of φ with $|\varphi| < \pi/2$. As we will discuss in Appendix A, this function has the expansion

$$\begin{aligned} &F(l,\varphi) \\ &= \frac{1}{2}\log(1 + e^{-l\sin\varphi}) - \frac{l}{2\pi}\left[\cos\varphi\left(\log\frac{1}{l} + 1 + \log\pi - \gamma_{\rm E}\right) + \left(\varphi - \frac{\pi}{2}\right)\sin\varphi\right] \\ &+ \sum_{k=1}^{\infty} \binom{-\frac{1}{2}}{k} \frac{1}{2k+1} \left(1 - \frac{1}{2^{2k+1}}\right) \zeta(2k+1) \cos\varphi \, {}_2F_1(-k, 1; \frac{1}{2} - k; \sin^2\varphi) \left(\frac{l}{\pi}\right)^{2k+1}. \end{aligned} \tag{5.11}$$

Using this expansion, we find the small l expansion of $A_{\rm extra}$,

$$\begin{aligned} A_{\rm extra} = &-\frac{1}{4} l \cos\phi \log(1+e^{-l\sin\phi}) - \frac{1}{4} l \sin\phi \log(1+e^{-l\cos\phi}) \\ &+ \frac{l^2}{4\pi}\left(\log\frac{1}{l} + 1 + \log\pi - \gamma_{\rm E} - \frac{\pi}{2}\cos\phi\sin\phi\right) \\ &- \pi \sum_{k=1}^{\infty} \binom{\frac{1}{2}}{k+1} \left(1 - \frac{1}{2^{2k+1}}\right) \zeta(2k+1) \frac{k+1}{2k+1} f_k(\phi) \left(\frac{l}{\pi}\right)^{2k+2}, \end{aligned} \tag{5.12}$$

where the function $f_k(\phi)$ is expressed in terms of the hypergeometric functions,

$$f_k(\phi) \equiv \cos^2\phi \, {}_2F_1(-k, 1; \frac{1}{2} - k; \sin^2\phi) + \sin^2\phi \, {}_2F_1(-k, 1; \frac{1}{2} - k; \cos^2\phi). \tag{5.13}$$

Combining (5.5), (5.8) and (5.12), we obtain the expression,

$$\begin{aligned} R_8 = &\frac{5\pi}{4} - \frac{1}{2}\log\left(2\cosh\frac{l\cos\phi}{2}\right)\log\left(2\cosh\frac{l\sin\phi}{2}\right) + \frac{l^2}{8\pi} \\ &+ \pi \sum_{k=1}^{\infty} \binom{\frac{1}{2}}{k+1} \left(1 - \frac{1}{2^{2k+1}}\right) \zeta(2k+1) \left(1 - \frac{k+1}{2k+1} f_k(\phi)\right) \left(\frac{l}{\pi}\right)^{2k+2}. \end{aligned} \tag{5.14}$$

Note that the non-analytic terms in (5.8) and (5.12) cancel each other out. The expression (5.14) is convergent for $|l| < \pi$. One can immediately confirm that the remainder function is expanded in l^2:

$$R_8 = \sum_{k=0}^{\infty} R_8^{(2k)}(\phi) l^{2k}, \tag{5.15}$$

where the first four coefficients are given by

$$R_8^{(0)}(\phi) = \frac{5\pi}{4} - \frac{\log^2 2}{2}, \tag{5.16}$$

$$R_8^{(2)}(\phi) = \frac{1}{8\pi} - \frac{\log 2}{16}, \tag{5.17}$$

$$R_8^{(4)}(\phi) = \frac{2\log 2 - 1}{1024} + \left(\frac{2\log 2 + 3}{3072} - \frac{7\zeta(3)}{192\pi^3}\right)\cos 4\phi, \tag{5.18}$$

$$R_8^{(6)}(\phi) = \frac{-8\log 2 + 3}{73728} - \left(\frac{8\log 2 + 5}{122880} - \frac{31\zeta(5)}{1280\pi^5}\right)\cos 4\phi. \tag{5.19}$$

We note that these maintain the symmetries $\phi \to -\phi$ and $\phi \to \phi + \frac{\pi}{2}$, which are due to the space-time parity and cyclicity [6]. The expansion (5.12) was derived for $0 < \phi < \pi/2$, but is valid for arbitrary ϕ due to these symmetries. In section 7, we will compare these results with the remainder function at two loops.

6. High-temperature expansion for the decagon

In the previous section, we have considered the remainder function for the octagon, and have obtained its all-order expansion with respect to the mass scale parameter l. The crucial point there is that the TBA system for the octagon is trivial. For the general $2\tilde{n}$-gon ($\tilde{n} \geq 5$), however, analytic solutions of the TBA equations have not been known yet. In this section, we consider the second simplest case $\tilde{n} = 5$: the decagon, and see how to compute the high-temperature expansion of its remainder function. Here, the underlying integrable theory is the homogeneous sine-Gordon model associated with the $\mathrm{SU}(3)_2/\mathrm{U}(1)^2$ coset CFT.

The remainder function for the decagon is divided into the following parts,

$$R_{10} = \frac{7}{4}\pi + A_{\text{periods}} + A_{\text{free}} + \Delta A_{\text{BDS}}. \tag{6.1}$$

The period part is given by

$$A_{\text{periods}} = -\frac{1}{4}(m_1\bar{m}_2 + m_2\bar{m}_1) = -\frac{1}{2}\tilde{M}_1\tilde{M}_2 l^2 \cos(\varphi_1 - \varphi_2), \tag{6.2}$$

where $m_j = M_j L e^{i\varphi_j}$, $\tilde{M}_j = M_j/M$ and $l = ML$. The free energy part is written as

$$A_{\text{free}} = \sum_{j=1}^{2} \int_{-\infty}^{\infty} \frac{d\theta}{2\pi} M_j L \cosh\theta \log(1 + \tilde{Y}_j(\theta)), \tag{6.3}$$

where $\tilde{Y}_j(\theta)$ is defined in (2.15). From (2.25), the part ΔA_{BDS} is given by

$$\Delta A_{\text{BDS}} = \frac{1}{4}\sum_{i,j=1}^{5} \log\frac{c^+_{i,j}}{c^+_{i,j+1}} \log\frac{c^-_{i-1,j}}{c^-_{i,j}}. \tag{6.4}$$

For the decagon, there are four independent cross-ratios. This is consistent with the fact that the TBA system has two independent complex parameters m_j ($j = 1, 2$). The cross-ratios $c^\pm_{13}$ and $c^\pm_{14}$ are related to the Y-functions,

$$c^-_{13} = Y_1(0), \qquad c^+_{13} = Y_1\left(-\frac{\pi i}{2}\right), \tag{6.5}$$

$$c^+_{14} = Y_2(0), \qquad c^-_{14} = Y_2\left(\frac{\pi i}{2}\right). \tag{6.6}$$

The other cross-ratios $c^\pm_{24}$, $c^\pm_{25}$ and $c^\pm_{35}$ are expressed by $c^\pm_{13}$ and $c^\pm_{14}$,

$$c^\pm_{24} = \frac{1 + c^\pm_{14}}{c^\pm_{13}}, \quad c^\pm_{35} = \frac{1 + c^\pm_{13}}{c^\pm_{14}}, \quad c^\pm_{25} = \left(1 + \frac{1}{c^\pm_{13}}\right)\left(1 + \frac{1}{c^\pm_{14}}\right) - 1. \tag{6.7}$$

Our goal is to find the small l behaviors of the remainder function.

6.1. Case with real masses

Let us start by restricting our attention to the case that two masses are real: $\varphi_1 = \varphi_2 = 0$. In this case, we can directly use the results of the CPT in section 4. The period term is

$$A_{\text{periods}} = -\frac{1}{2}\tilde{M}_1\tilde{M}_2 l^2. \tag{6.8}$$

Let us consider the free energy part. Since the central charge of the $\mathrm{SU}(3)_2/\mathrm{U}(1)^2$ coset CFT is $c_3 = 6/5$, the free energy goes to $\pi/5$ in the limit $(m_1, m_2) \to (0, 0)$. The perturbing operator has the dimension $\Delta = \bar{\Delta} = 3/5$. From (3.24), the bulk term is given by

$$f_3^{\text{bulk}} = \frac{1}{2}\tilde{M}_1\tilde{M}_2 l^2. \tag{6.9}$$

Thus the free energy has the following expansion,

$$A_{\text{free}} = \frac{\pi}{5} + \frac{1}{2}\tilde{M}_1\tilde{M}_2 l^2 + \sum_{k=2}^{\infty} f_3^{(k)} l^{4k/5}, \tag{6.10}$$

where $f_3^{(k)}$ is computed by the CPT (see (3.22)). In particular, $f_3^{(2)}$ is read from (3.27):

$$f_3^{(2)} = \frac{\pi}{6}\kappa_3^2 G^2(\tilde{M}_1, \tilde{M}_2) C_3^{(2)}, \quad C_3^{(2)} = 3(2\pi)^{\frac{4}{5}}\gamma^2\Big(\frac{3}{5}\Big)\gamma\Big(-\frac{1}{5}\Big), \tag{6.11}$$

where $\gamma(x) = \Gamma(x)/\Gamma(1-x)$ and

$$G(\tilde{M}_1, \tilde{M}_2) = \sum_{i,j=1}^{2} \tilde{M}_i^{2/5} F_{ij} \tilde{M}_j^{2/5}. \tag{6.12}$$

We need to determine the symmetric matrix F, which has two independent components for the decagon. In principle, it should be possible to fix them by considering the quantum theory of the $\mathrm{SU}(3)_2/\mathrm{U}(1)^2$ HSG model. However, we take a different strategy here. Fortunately, we can completely fix F_{ij} by the following consideration in the case of the decagon.

Let us first take the limit $(M_1, M_2) \to (M, 0)$. In this limit, the TBA equations for the decagon reduce to those for the $(\mathrm{RSOS})_3$ scattering theory. Therefore the correction (6.11) should be equal to that for the $(\mathrm{RSOS})_3$ scattering theory,[7] and we

[7]Since the $(\mathrm{RSOS})_3$ model has the central charge $c = 7/10$, the free energy goes to $7\pi/60$ in the limit $ML \to 0$. The difference of the constant terms of the free energies in two theories comes from the fact that the contribution of particle 2 is absent in the $(\mathrm{RSOS})_3$ scattering theory. One can numerically check that in the homogeneous sine-Gordon model, the contributions of particles 1 and 2 go to $7\pi/60$ and $\pi/12$, respectively in the limit $ML \to 0$ with $\tilde{M}_2 \ll \tilde{M}_1 = 1$, and the sum of two-particle contributions gives the correct value $\pi/5$. Furthermore all the high-temperature corrections of particle 2 should vanish if we take the limit $M_2 \to 0$.

obtain

$$F_{11}\kappa_3 = \kappa_3^{\mathrm{RSOS}}, \tag{6.13}$$

where κ_3^{RSOS} is given by (3.33).

Let us next consider the case: $M_1 = M_2 = M$. In this case, the TBA equations are regarded as those associated with the tadpole Dynkin diagram T_1. The corresponding integrable model is the non-unitary $(\mathrm{SU}(2)_{-1/2} \times \mathrm{SU}(2)_1)/\mathrm{SU}(2)_{1/2}$ coset model perturbed by the primary field $\phi_{1,1,3}$ with dimension $\Delta = \bar{\Delta} = 3/5$ (see subsection 3.2). We discuss the perturbation of the above coset model in Appendix B. Using the result (B.10), we find the constraint

$$\frac{2\pi}{3}\kappa_3^2(F_{11}+F_{12})^2 C_3^{(2)} = \frac{1}{8}\left(\frac{\pi}{4}\right)^{1/5}\gamma\left(\frac{1}{4}\right)^{8/5}\gamma\left(-\frac{1}{5}\right)\gamma\left(\frac{3}{5}\right)\gamma\left(\frac{4}{5}\right). \tag{6.14}$$

Combining (6.13) and (6.14), we obtain

$$1 + \frac{F_{12}}{F_{11}} = \frac{1}{2}\left(\frac{3}{\pi^2}\right)^{1/5}\gamma\left(\frac{1}{4}\right)^{4/5}. \tag{6.15}$$

From these two considerations, the order $l^{8/5}$ correction of the free energy must have the following form

$$f_3^{(2)} = f_{(\mathrm{RSOS})_3}^{(2)} F_{11}^{-2} G^2(\tilde{M}_1, \tilde{M}_2) \tag{6.16}$$

where

$$f_{(\mathrm{RSOS})_3}^{(2)} = \frac{\pi}{6}(\kappa_3^{\mathrm{RSOS}})^2 C_3^{(2)} = \frac{\pi}{8\cdot 6^{2/5}}\gamma\left(-\frac{1}{5}\right)\gamma\left(\frac{3}{5}\right)\gamma\left(\frac{4}{5}\right), \tag{6.17}$$

and

$$F_{11}^{-1} G(\tilde{M}_1, \tilde{M}_2) = \tilde{M}_1^{4/5} + \tilde{M}_2^{4/5} - B\tilde{M}_1^{2/5}\tilde{M}_2^{2/5}, \tag{6.18}$$

$$B = -\frac{2F_{12}}{F_{11}} = 2 - \left(\frac{3}{\pi^2}\right)^{1/5}\gamma\left(\frac{1}{4}\right)^{4/5}. \tag{6.19}$$

As seen in section 3, the matrix F deviates from the inverse of the Cartan matrix. We have confirmed that (6.16) is in good agreement with the numerical results for arbitrary $\tilde{M}_1$ and $\tilde{M}_2$ (Fig. 1).

Now we proceed to the expansion of ΔA_{BDS}. In order to know the small l behavior of ΔA_{BDS}, we need the high-temperature expansions of the Y-functions. Since the

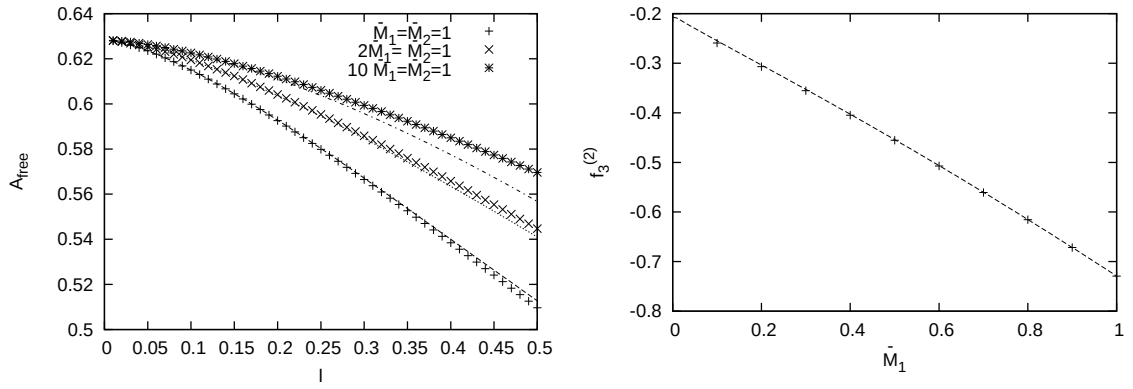

(a) (b)

Figure 1: (a) The scale parameter l-dependence of the free energy with fixed $\tilde{M}_1/\tilde{M}_2 = 1, 1/2$ and $1/10$. Dashed lines represent the curve $\frac{\pi}{5} + \frac{1}{2}\tilde{M}_1\tilde{M}_2 l^2 + f_3^{(2)} l^{8/5}$. Deviation from the analytic formula at $l = 0.5$ for $\tilde{M}_1/\tilde{M}_2 = 1/10$ comes from the next order correction $O(l^{12/5})$, which is estimated from the numerical fit as $0.08 l^{12/5} \approx 0.015$. (b) $\tilde{M}_1$-dependence of the coefficient of $l^{8/5}$ of the free energy for $\tilde{M}_2 = 1$. Dashed line corresponds to the curve $f_3^{(2)}$ given in (6.16).

Y-functions are related to the T-functions, we can use the results in section 4. In the decagon case, the relations between Y_j and T_j are as follows,

$$Y_1(\theta) = T_2(\theta), \quad Y_2(\theta) = T_1(\theta). \tag{6.20}$$

As in (4.19) and (4.27), the high-temperature expansions of the T-functions are computed from the data of the g-functions at the CFT point. Using the formula (4.30) of the modular S-matrix, one obtains

$$\frac{g_{|1\rangle}}{g_{|\mathbb{1}\rangle}} = \frac{g_{|2\rangle}}{g_{|\mathbb{1}\rangle}} = 2\cos\left(\frac{\pi}{5}\right), \quad \frac{g^{\Phi}_{|\mathbb{1}\rangle}}{g_{|\mathbb{1}\rangle}} = G(\tilde{M}_1, \tilde{M}_2)\left[2\cos\left(\frac{\pi}{5}\right)\right]^{1/2}, \tag{6.21}$$

$$\frac{g^{\Phi}_{|1\rangle}}{g_{|1\rangle}} = \frac{g^{\Phi}_{|2\rangle}}{g_{|2\rangle}} = -G(\tilde{M}_1, \tilde{M}_2)\left[2\cos\left(\frac{\pi}{5}\right)\right]^{-3/2}, \tag{6.22}$$

Therefore from (4.26), we find

$$Y_j(\theta) = Y^{(0)} + Y^{(2)}(\tilde{M}_1, \tilde{M}_2) l^{4/5} \cosh\left(\frac{4\theta}{5}\right) + \mathcal{O}(l^{6/5}), \tag{6.23}$$

where

$$Y^{(0)} = 2\cos\left(\frac{\pi}{5}\right), \tag{6.24}$$

and

$$Y^{(2)}(\tilde{M}_1, \tilde{M}_2) = y^{(2)}_{(\mathrm{RSOS})_3} F_{11}^{-1} G(\tilde{M}_1, \tilde{M}_2) \tag{6.25}$$

$$y^{(2)}_{(\mathrm{RSOS})_3} = \frac{1}{4 \cdot 6^{1/5}} \Gamma\left(-\frac{1}{5}\right) \left[10 \cos\left(\frac{\pi}{5}\right) \gamma\left(\frac{3}{5}\right) \gamma\left(\frac{4}{5}\right)\right]^{1/2}. \tag{6.26}$$

From (6.5) and (6.6), the cross-ratios are expanded as

$$c^-_{13} = c^+_{14} = Y^{(0)} + Y^{(2)} l^{4/5} + \mathcal{O}(l^{6/5}), \tag{6.27}$$

$$c^+_{13} = c^-_{14} = Y^{(0)} + Y^{(2)} l^{4/5} \cos\left(\frac{2}{5}\pi\right) + \mathcal{O}(l^{6/5}). \tag{6.28}$$

As shown in Appendix D, the expansion of the ΔA_{BDS} is largely constrained by the Y-system, the structure of the conformal perturbation, as well as the symmetries associated with the space-time parity and cyclicity, under which ΔA_{BDS} is invariant. Consequently, it turns out that the terms of $\mathcal{O}(l^{4/5})$ are enough to give the expansion of ΔA_{BDS} up to $\mathcal{O}(l^{12/5})$. We then obtain the high-temperature expansion of ΔA_{BDS},

$$\Delta A_{\mathrm{BDS}} = -\frac{5}{2} \log^2\left(2 \cos\left(\frac{\pi}{5}\right)\right) + B_2 (Y^{(2)})^2 l^{8/5} + \mathcal{O}(l^{12/5}), \tag{6.29}$$

where B_2 is given by

$$B_2 = 20 \cos^4\left(\frac{2\pi}{5}\right) \left(1 - \frac{1}{\sqrt{5}} \log\left(2 \cos\left(\frac{\pi}{5}\right)\right)\right). \tag{6.30}$$

Note that the first order term $\mathcal{O}(l^{4/5})$ vanishes. In summary, from (6.8), (6.10), (6.16) and (6.29), the remainder function with the real masses has the following expansion,

$$R_{10} = R^{(0)}_{10} + R^{(4)}_{10} l^{8/5} + \mathcal{O}(l^{12/5}), \tag{6.31}$$

where

$$R^{(0)}_{10} = \frac{39}{20}\pi - \frac{5}{2} \log^2\left(2 \cos\left(\frac{\pi}{5}\right)\right), \tag{6.32}$$

$$R^{(4)}_{10} = \left(-\frac{1}{5} \tan\left(\frac{\pi}{5}\right) + B_2\right) Y^{(2)}(\tilde{M}_1, \tilde{M}_2)^2. \tag{6.33}$$

Note that A_{periods} is canceled by the bulk term in the free energy, and the remainder function is expanded in $l^{2/5}$. We also comment that the ratio $f^{(2)}_{(\mathrm{RSOS})_3}/(y^{(2)}_{(\mathrm{RSOS})_3})^2$ interestingly becomes very simple,

$$\frac{f^{(2)}_{(\mathrm{RSOS})_3}}{(y^{(2)}_{(\mathrm{RSOS})_3})^2} = -\frac{1}{5} \tan\left(\frac{\pi}{5}\right). \tag{6.34}$$

6.2. Case with complex masses

So far, we have focused on the case that two masses are real. We would now like to discuss the general situation where two masses are complex. The phase of the complex mass corresponds to the purely imaginary resonance parameter. As discussed in section 3, it is not clear if this case can be treated within the framework of the conformal perturbation of the HSG model. However, one can expect that the expansion is analytic in the mass parameters [46], and the expansion for the real masses can be extended to that for the complex masses by continuing the mass parameters. This is also expected from the point of view of the TBA equations. In fact, we will see that the results obtained in this way are in agreement with numerical computations. Furthermore, one can arrive at the same conclusion for some relevant quantities by considering the chiral limit of the TBA system, which is discussed in detail in Appendix C.

The way to incorporate the phase is determined by the the following facts: the resonance parameters in the TBA equations are understood as due to the rescaling of the mass parameters, the free energy, by definition, should depend only on the difference of the phases $\varphi_{12} = \varphi_1 - \varphi_2$, and $\boldsymbol{\lambda}, \bar{\boldsymbol{\lambda}}$ are of the form (3.3) semi-classically. We thus make a replacement, in the complex mass case,

$$\boldsymbol{\lambda} \to \sum_j (\tilde{M}_j e^{i\varphi_j})^{1-(\Delta+\bar{\Delta})/2} \hat{\boldsymbol{\lambda}}_j, \tag{6.35}$$

$$\bar{\boldsymbol{\lambda}} \to \sum_j (\tilde{M}_j e^{-i\varphi_j})^{1-(\Delta+\bar{\Delta})/2} \hat{\boldsymbol{\lambda}}_j. \tag{6.36}$$

Then the two-point function of the perturbing operator becomes

$$\left\langle \Phi_{\boldsymbol{\lambda},\bar{\boldsymbol{\lambda}}}(z) \Phi_{\boldsymbol{\lambda},\bar{\boldsymbol{\lambda}}}(0) \right\rangle = \frac{\left| G(\tilde{M}_1 e^{i\varphi_1}, \tilde{M}_2 e^{i\varphi_2}) \right|^2}{|z|^{12/5}}, \tag{6.37}$$

where G is given by (6.18).

Let us consider the free energy. As mentioned above, the free energy must be a function of φ_{12}. This suggests that the bulk term is modified as

$$f_3^{\text{bulk}} \to \frac{1}{4} l^2 \sum_{i,j=1}^{2} (\tilde{M}_i e^{i\varphi_i})(I^{-1})_{ij} (\tilde{M}_j e^{-i\varphi_j}) = \frac{1}{2} \tilde{M}_1 \tilde{M}_2 l^2 \cos\varphi_{12}. \tag{6.38}$$

Taking into account these modifications, we find that the expansion of the free energy is given by

$$A_{\text{free}} = \frac{\pi}{5} + \frac{1}{2} \tilde{M}_1 \tilde{M}_2 l^2 \cos\varphi_{12} + f^{(2)}_{(\text{RSOS})_3} F_{11}^{-2} \left| G(\tilde{M}_1 e^{i\varphi_1}, \tilde{M}_2 e^{i\varphi_2}) \right|^2 l^{8/5} + \mathcal{O}(l^{12/5}). \tag{6.39}$$

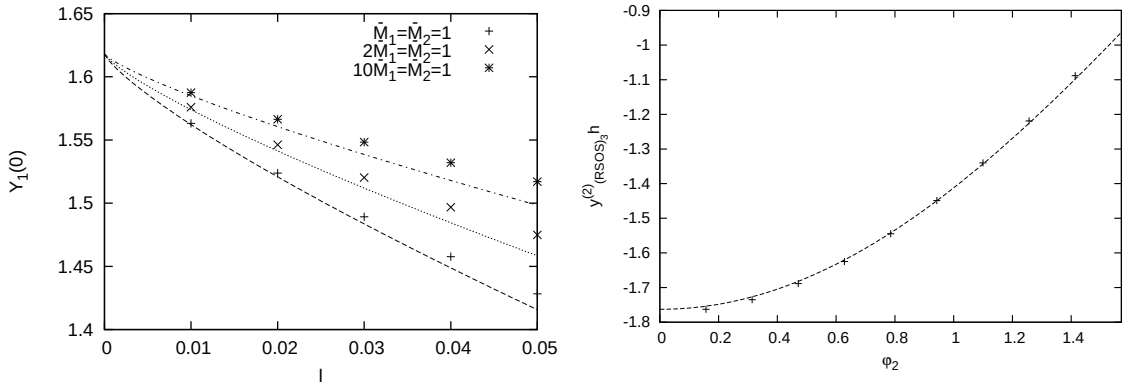

(a) (b)

Figure 2: (a) The l-dependence of the Y-function $Y_1(0)$ for fixed $\tilde{M}_1/\tilde{M}_2 = 1, 1/2$ and $1/10$ at $\varphi_1 = \varphi_2 = \pi/20$. Dashed lines represent the curve (6.40) at $\theta = 0$ up to the order $l^{4/5}$. Deviation from the analytic formula comes from the next order correction $O(l^{6/5})$, which can be estimated from the numerical fit as $0.15l^{6/5} \approx 0.004$ ($l = 0.05$) for $\tilde{M}_1 = \tilde{M}_2 = 1$. (b) Plots of the coefficient of $l^{4/5}$ in $Y_1(0)$ for $\varphi_1 = \pi/20$ and various φ_2 at $2\tilde{M}_1 = \tilde{M}_2 = 1$. Dashed line represents the curve $\frac{1}{2}\big(Y^{(2)}(\tilde{M}_1 e^{-i\varphi_1}, \tilde{M}_2 e^{-i\varphi_2}) + Y^{(2)}(\tilde{M}_1 e^{i\varphi_1}, \tilde{M}_2 e^{i\varphi_2})\big) =: y^{(2)}_{(\mathrm{RSOS})_3} h(\tilde{M}_j, \varphi_j)$.

The relation between the g- and T-functions in section 4 is not applied to the case of complex masses. However, by similarly complexifying the mass parameters, we obtain the expansion of the Y-functions,

$$Y_j(\theta) = 2\cos\left(\frac{\pi}{5}\right) + \frac{1}{2}\Big(Y^{(2)}(\tilde{M}_1 e^{-i\varphi_1}, \tilde{M}_2 e^{-i\varphi_2}) e^{4\theta/5} + Y^{(2)}(\tilde{M}_1 e^{i\varphi_1}, \tilde{M}_2 e^{i\varphi_2}) e^{-4\theta/5}\Big) l^{4/5} + \mathcal{O}(l^{6/5}), \tag{6.40}$$

where $Y^{(2)}$ is given by (6.25). We have checked that this formula agrees with the numerical results (Fig. 2). The expansion of the Y-functions for the complex masses is also discussed in Appendix C from the chiral limit of the TBA system. The space-time cross-ratios are again obtained by using the relations (6.5) and (6.6). In addition, using (6.40), the expansion of ΔA_{BDS} is given as in the case of the real masses by

$$\Delta A_{\mathrm{BDS}} = -\frac{5}{2}\log^2\left(2\cos\left(\frac{\pi}{5}\right)\right) + B_2\big|Y^{(2)}(\tilde{M}_1 e^{i\varphi_1}, \tilde{M}_2 e^{i\varphi_2})\big|^2 l^{8/5} + \mathcal{O}(l^{12/5}). \tag{6.41}$$

Collecting all the above results, we finally find that the remainder function with the complex masses has the expansion,

$$R_{10} = R_{10}^{(0)} + R_{10}^{(4)} l^{8/5} + \mathcal{O}(l^{12/5}), \tag{6.42}$$

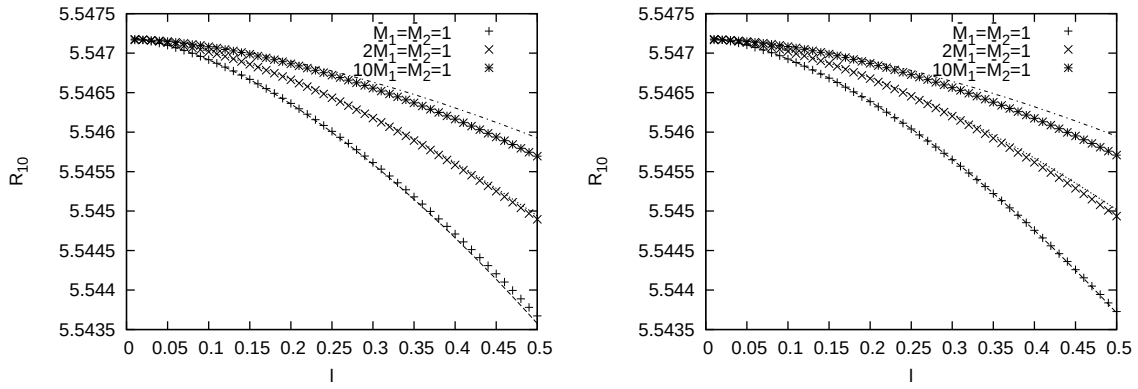

(a) (b)

Figure 3: The l-dependence of the remainder function with (a) equal phase $\varphi_1 = \varphi_2 = \pi/20$ (b) different phase $\varphi_1 = \pi/20$, $\varphi_2 = \pi/5$. Dashed lines represent the curve $R_{10}^{(0)} + R_{10}^{(4)} l^{8/5}$.

where

$$R_{10}^{(0)} = \frac{39}{20}\pi - \frac{5}{2}\log^2\left(2\cos\left(\frac{\pi}{5}\right)\right), \tag{6.43}$$

$$R_{10}^{(4)} = \left(-\frac{1}{5}\tan\left(\frac{\pi}{5}\right) + B_2\right)\left|Y^{(2)}(\tilde{M}_1 e^{i\varphi_1}, \tilde{M}_2 e^{i\varphi_2})\right|^2. \tag{6.44}$$

$Y^{(2)}$ and B_2 are defined by (6.25) and (6.30), respectively. Note that the A_{periods} is canceled by the bulk term of the free energy again. We have confirmed that this formula for R_{10} is in good agreement with the numerical results for various values of $\tilde{M}_{1,2}$ and $\varphi_{1,2}$ (Fig. 3).

At the end of this section, we comment on the relation between cross-ratios and the parameters in the TBA system. In order to express the remainder function as a function of the cross-ratios, one has to invert the relations (6.5) and (6.6). This is complicated for general complex masses. However, when the phases of m_j are equal, i.e., $\varphi_j = \varphi$, $Y_j(\theta)$ are obtained from those for the real masses by the shift $\theta \to \theta - \varphi$. One then simply has

$$\frac{4}{5}\varphi = \tan^{-1}\left(\cot\left(\frac{2}{5}\pi\right)\frac{\delta c_{14}^- - \delta c_{13}^+}{\delta c_{14}^- + \delta c_{13}^+}\right), \quad Y^{(2)} l^{4/5} = \frac{\delta c_{13}^+}{\cos\left(\frac{2}{5}(\pi + 2\varphi)\right)}, \tag{6.45}$$

where $\delta c_{jk}^{\pm} := c_{jk}^{\pm} - Y^{(0)}$. Of course, one has to keep in mind that these expressions are valid for small l. This corresponds to focusing on the kinematics near $c_{13}^+ = c_{13}^- = c_{14}^+ = c_{14}^-$ in the space of the cross-ratios (or equivalently near the regular decagon).

7. Comparison with two-loop results

Wilson loops with light-like edges are dual to gluon scattering amplitudes [2]. For the kinematic configurations corresponding to the AdS_3 octagon, the analytic expression of the 2-loop remainder function for the Wilson loop is given in [19]. The analytic expression for the case of AdS_3 $2n$-gon has also been written down [20, 21]. In this section, we compare our strong coupling results with those at two loops as expansions around the kinematic configurations associated with regular polygons.

7.1. Octagon

In the case of the octagon, the remainder function at two loops is[8]

$$R_8^{\text{2-loop}} = -\frac{\pi^4}{18} - \frac{1}{2}\log(1+\chi^+)\log\left(1+\frac{1}{\chi^+}\right)\log(1+\chi^-)\log\left(1+\frac{1}{\chi^-}\right), \quad (7.1)$$

where the cross-ratios $\chi^\pm$ are given in (5.6). Similarly to the strong coupling case, this is expanded by using (A.10) as

$$R_8^{\text{2-loop}} = \sum_{k=0}^{\infty} R_8^{\text{2-loop}\,(2k)}(\phi)\, l^{2k}, \quad (7.2)$$

where the first few coefficients are

$$\begin{aligned} R_8^{\text{2-loop}\,(0)}(\phi) &= -\frac{\pi^4}{18} - \frac{\log^4 2}{2}, \\ R_8^{\text{2-loop}\,(2)}(\phi) &= -\frac{\log^2 2(\log 2 - 1)}{8}, \\ R_8^{\text{2-loop}\,(4)}(\phi) &= \frac{2\log^3 2 - 5\log^2 2 + 4\log 2 - 2}{512} \\ &\quad + \frac{2\log^3 2 + 3\log^2 2 - 12\log 2 + 6}{1536}\cos 4\phi. \end{aligned} \quad (7.3)$$

One can check that $R_8^{\text{2-loop}\,(0)}$ agrees with $R_8^{\text{2-loop}}$ for the regular octagon [19], and that the coefficients $R_8^{\text{2-loop}\,(2k)}$ maintain the space-time parity and cyclicity.

For comparison of the results at strong coupling and at two loops, we introduce rescaled remainder functions [52]. For the AdS_3 $2n$-gon, they are defined by

$$\bar{R}_{2n} := \frac{R_{2n} - R_{2n,\text{reg}}}{R_{2n,\text{reg}} - (n-2)R_{6,\text{reg}}}, \quad (7.4)$$

at strong coupling, and a similar expression at two loops, where $R_{2n,\text{reg}}$ stands for the remainder function for the regular $2n$-gon. Since R_{2n}, $R_{2n}^{\text{2-loop}}$ reduce to superpositions

[8] The overall coupling dependence is suppressed.

of the contributions from $(n-2)$ regular hexagons in the low-temperature/collinear limit [6, 20], the rescaled remainder functions are calibrated to take -1 in this limit. It has been observed numerically [19, 52] that $\bar{R}_8$ at strong coupling and $\bar{R}_8^{\text{2-loop}}$ at two loops are very similar.

Given (5.15) and (7.2), we are now able to derive analytic expansions of $\bar{R}_8$ and $\bar{R}_8^{\text{2-loop}}$. By noting that the remainder functions for the regular hexagon and octagon are

$$R_{6,\text{reg}} = \frac{7\pi}{12}, \quad R_{8,\text{reg}} = R_8^{(0)}, \tag{7.5}$$

and

$$R_{6,\text{reg}}^{\text{2-loop}} = -\frac{\pi^4}{36}, \quad R_{8,\text{reg}}^{\text{2-loop}} = R_8^{\text{2-loop}\,(0)}, \tag{7.6}$$

respectively, we obtain

$$\bar{R}_8 = \sum_{k=1}^{\infty} \bar{R}_8^{(2k)}(\phi) l^{2k}, \qquad \bar{R}_8^{\text{2-loop}} = \sum_{k=1}^{\infty} \bar{R}_8^{\text{2-loop}\,(2k)}(\phi) l^{2k} \tag{7.7}$$

where the first few coefficients at strong coupling are

$$\begin{aligned} \bar{R}_8^{(2)}(\phi) &= \frac{\frac{1}{8\pi} - \frac{\log 2}{16}}{\frac{\pi}{12} - \frac{\log^2 2}{2}} \approx -0.1637687, \\ \bar{R}_8^{(4)}(\phi) &\approx 0.0174868 + 0.000667828 \cos 4\phi, \\ \bar{R}_8^{(6)}(\phi) &\approx -0.00160021 - 0.000173979 \cos 4\phi, \end{aligned} \tag{7.8}$$

whereas those at two loops are

$$\begin{aligned} \bar{R}_8^{\text{2-loop}(2)}(\phi) &= \frac{\log 2 - 1}{4 \log^2 2} \approx -0.15966848, \\ \bar{R}_8^{\text{2-loop}(4)}(\phi) &\approx 0.0163067 + 0.00118658 \cos 4\phi, \\ \bar{R}_8^{\text{2-loop}(6)}(\phi) &\approx -0.00141679 - 0.00029145 \cos 4\phi. \end{aligned} \tag{7.9}$$

We observe that they are indeed close to each other (but different).

7.2. Decagon

Let us move on to a discussion on the AdS_3 decagon. In this case, the analytic expression of the remainder function in [20, 21] is

$$R_{10}^{\text{2-loop}} = -\frac{\pi^4}{12} - \frac{1}{2} \sum_{k=1}^{10} \log(u_k) \log(u_{k+1}) \log(u_{k+2}) \log(u_{k+3}) \,, \tag{7.10}$$

with $u_k = u_{k+10}$. The cross-ratios u_k are related to $c_{13}^{\pm}, c_{14}^{\pm}$ by[9]

$$\begin{aligned}
u_{10} &= \frac{1+c_{13}^{+}}{1+c_{13}^{+}+c_{14}^{+}}\,, & u_1 &= \frac{1+c_{13}^{-}}{1+c_{13}^{-}+c_{14}^{-}}\,,\\
u_2 &= \frac{c_{14}^{+}}{c_{14}^{+}+1}\,, & u_3 &= \frac{c_{14}^{-}}{c_{14}^{-}+1}\,,\\
u_4 &= \frac{1+c_{13}^{+}+c_{14}^{+}}{(1+c_{13}^{+})(1+c_{14}^{+})}\,, & u_5 &= \frac{1+c_{13}^{-}+c_{14}^{-}}{(1+c_{13}^{-})(1+c_{14}^{-})}\,,\\
u_6 &= \frac{c_{13}^{+}}{c_{13}^{+}+1}\,, & u_7 &= \frac{c_{13}^{-}}{c_{13}^{-}+1}\,,\\
u_8 &= \frac{1+c_{14}^{+}}{1+c_{13}^{+}+c_{14}^{+}}\,, & u_9 &= \frac{1+c_{14}^{-}}{1+c_{13}^{-}+c_{14}^{-}}\,.
\end{aligned} \tag{7.11}$$

Since $R_{10}^{\text{2-loop}}$ is invariant under the symmetries associated with the space-time parity and cyclicity, its high-temperature expansion is largely constrained similarly to ΔA_{BDS}. Consequently, by substituting the cross-ratios (6.5), (6.6) into (7.10), (7.11), one obtains the following expansion of the remainder function at two loops:

$$R_{10}^{\text{2-loop}} = \sum_{k=0}^{\infty} R_{10}^{\text{2-loop}\,(k)}\, l^{2k/5}\,, \tag{7.12}$$

where the first few coefficients are

$$\begin{aligned}
R_{10}^{\text{2-loop}\,(0)} &= -\frac{\pi^4}{12} - 5\log^4\!\big(2\cos\frac{\pi}{5}\big),\\
R_{10}^{\text{2-loop}\,(1)} &= R_{10}^{\text{2-loop}\,(2)} = R_{10}^{\text{2-loop}\,(3)} = 0,\\
R_{10}^{\text{2-loop}\,(4)} &= D_2 \cdot \big|Y^{(2)}(\tilde{M}_1 e^{i\varphi_1}, \tilde{M}_2 e^{i\varphi_2})\big|^2,
\end{aligned} \tag{7.13}$$

with

$$D_2 = 2^4\sqrt{5}\cos^6\!\Big(\frac{2\pi}{5}\Big)\log^2\!\Big(2\cos\frac{\pi}{5}\Big)\Big[3\sqrt{5} - 2^4\cos^2\!\Big(\frac{\pi}{5}\Big)\log\!\Big(2\cos\frac{\pi}{5}\Big)\Big]\,. \tag{7.14}$$

One can check that $R_{10}^{\text{2-loop}\,(0)}$ agrees with the numerical value of $R_{10}^{\text{2-loop}}$ for the regular decagon [52]. The structure of the expansion is very similar to that of R_{10} at strong coupling, which is understood as due to the space-time symmetries (see Appendix D for details.).

Given the above result, we can compare the rescaled remainder functions at strong coupling and at two loops. From (7.4) and a similar expression with

$$R_{10,\text{reg}} = R_{10}^{(0)}\,, \quad R_{10,\text{reg}}^{\text{2-loop}} = R_{10}^{\text{2-loop}\,(0)}\,, \tag{7.15}$$

[9]We identify $x_k^{\pm}$ in [20] with $x_k^{\mp}$, so that the $\mathbb{Z}_{10}$ symmetry from the parity and cyclicity matches at strong coupling and at two loops.

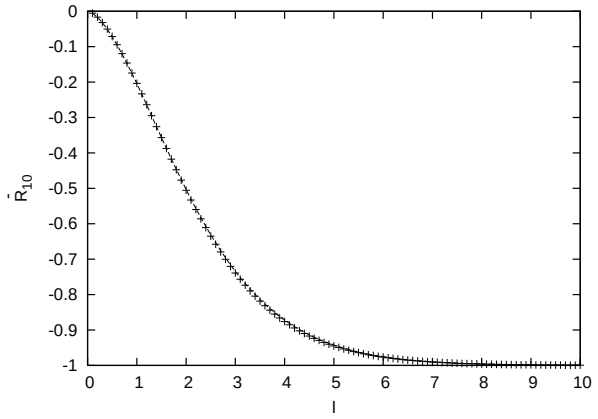

Figure 4: Plots of the l-dependence of the rescaled remainder functions at strong coupling (points) and at two loops (dashed lines). The functions are evaluated at $\tilde{M}_1 = \tilde{M}_2 = 1$ and $\varphi_1 = \varphi_2 = \pi/20$.

we find that

$$\begin{aligned}\bar{R}_{10} &= \bar{C}_{8/5} \left|Y^{(2)}(\tilde{M}_1 e^{i\varphi_1}, \tilde{M}_2 e^{i\varphi_2})\right|^2 \cdot l^{8/5} + \mathcal{O}(l^{12/5}) \,, \\ \bar{R}_{10}^{\text{2-loop}} &= \bar{C}_{8/5}^{\text{2-loop}} \left|Y^{(2)}(\tilde{M}_1 e^{i\varphi_1}, \tilde{M}_2 e^{i\varphi_2})\right|^2 \cdot l^{8/5} + \mathcal{O}(l^{12/5}) \,, \end{aligned} \tag{7.16}$$

where

$$\begin{aligned}\bar{C}_{\frac{8}{5}} &= \frac{-\frac{1}{5}\tan\frac{\pi}{5} + B_2}{\frac{\pi}{5} - \frac{5}{2}\log^2\left(2\cos\frac{\pi}{5}\right)} \approx -0.0441916 \,, \\ \bar{C}_{\frac{8}{5}}^{\text{2-loop}} &= \frac{-D_2}{5\log^4\left(2\cos\frac{\pi}{5}\right)} \approx -0.0449039 \,. \end{aligned} \tag{7.17}$$

B_2 and D_2 are given in (6.30) and (7.14), respectively. Again, we observe that they are very close. We note that the two functions are also very close for finite l (Fig. 4). This suggests that not only the high-temperature expansion but also the remainder function itself is strongly constrained by the Y-system and the space-time symmetries, in addition to the collinear limits [20, 21, 53].

8. Conclusions and discussion

In this paper we have studied the remainder functions of the gluon scattering amplitudes at strong coupling by using the integrable bulk and boundary perturbation of conformal field theory. In particular we have studied the minimal surfaces in AdS_3, which correspond to the Wilson loops with a $2\tilde{n}$-sided light-like polygonal boundary.

The minimal surface is described by the TBA system, and the related integrable model is the homogeneous sine-Gordon model with purely imaginary resonance parameters. This model is obtained by the integrable perturbation of generalized parafermions. We have investigated high-temperature (small mass) expansion of the free energy, the T-functions and Y-functions of this model, which give the remainder function around the kinematic configurations associated with regular polygons. The high-temperature expansion of the free energy is calculated by the bulk perturbation of the CFT. For the T-functions, we have introduced the g-functions whose ratios obey the same integral equations and asymptotic conditions. By using this relation, we have calculated the T-functions.

For the 8-point amplitudes (octagon), the relevant CFT is the critical Ising model. Since we know the exact g-function in this case, we have performed all-order high-temperature expansion of the remainder function. We have compared this result with the 2-loop remainder function, and have observed that the two results show similar power series expansions with very close coefficients.

We have also been able to obtain an explicit formula for the first order correction to the remainder function in the case of the 10-point amplitudes (decagon). The correction agrees with the numerical solution of the TBA equations for small masses. We have compared this result with the proposed 2-loop remainder function. Again, we have observed that the rescaled remainder functions have similar power series structures with close coefficients. This observed similarity suggests that their power series structure is strongly constrained by the Y-system and the space-time symmetries, in addition to the collinear limits [20, 21, 53].

The Y-functions are obtained from the cross-ratios of the T-functions. A notable observation in our discussion is that the T- and Y-functions in the CFT limit is given by the modular S-matrix through the g-functions. This suggests an interesting relation between the modular S-matrices and solutions of constant Y-systems, which are used to compute the central charge of CFT using the dilogarithm identities [10, 48, 49]. Although we have also observed that the same integral equations are derived from the g- and T-functions, the role of the boundary perturbation of CFT in the context of gluon scattering amplitudes is not quite clear at this moment. These points would deserve further investigations.

For future direction, it would be possible to extend our discussion to the cases of more than 10-point amplitudes, amplitudes with more general kinematic configurations corresponding to AdS_4 and AdS_5, and form factors [22]. For these purposes, it

would be important to understand multi-parameter integrable deformations of the generalized parafermionic CFT. In addition, the underlying integrable models/CFTs for the AdS_5 case are yet to be clarified. Taking into account the case of the AdS_5 hexagon [7, 13], one may expect them to be obtained by some deformation from the AdS_4 case [9]. Details should, however, be discussed further.

Regarding higher order expansions, the approach adopted in this paper requires higher correlation functions in the presence of both the bulk and the boundary deformations. In order to cover the full kinematic region of gluon momenta, one needs higher order expansion, which is connected to the low-temperature (large mass) region [7, 9, 53, 54]. On the other hand, a different approach to study the analytic expansion of the T-functions has been given by Bazhanov et al. for kink (massless) TBA systems (see Appendix C) [39,55]. For massive systems, see for example [56,57]. It would be interesting to apply this to the study of the minimal surface, as well as to understand the relation between these two approaches.

Acknowledgments

We would like to thank J. Suzuki and Z. Tsuboi for useful discussions and conversations, and R. Tateo for useful discussions and for pointing out the relation between the T- and g-functions to us. The work of K. S. and Y. S. is supported in part by Grant-in-Aid for Scientific Research from the Japan Ministry of Education, Culture, Sports, Science and Technology. The work of K. S. is also supported by Keio Gijuku Academic Development Funds.

Appendices

A. Expansion of $F(l, \varphi)$

In this appendix, we derive the high-temperature expansion of $F(l, \varphi)$ defined by (5.9). First we expand $F(l, \varphi)$ in $\sin \varphi$,

$$\begin{aligned} F(l,\varphi) &= \frac{\cos\varphi}{\pi}\int_0^\infty dt \frac{\cosh t}{\cosh^2 t - \sin^2\varphi}\log(1+e^{-l\cosh t}), \\ &= \frac{\cos\varphi}{\pi}\sum_{n=0}^{\infty}\sin^{2n}\varphi\,\Phi_{2n+1}(l), \end{aligned} \tag{A.1}$$

where

$$\Phi_m(l) \equiv \int_0^\infty \frac{dt}{\cosh^m t} \log(1+e^{-l\cosh t}) = \sum_{k=1}^\infty \frac{(-1)^{k-1}}{k} \int_0^\infty \frac{dt}{\cosh^m t} e^{-kl\cosh t}. \quad \text{(A.2)}$$

It is easy to see that the m-th derivative of $\Phi_m(l)$ is expressed in terms of the modified Bessel function of the second kind,

$$\Phi_m^{(m)}(l) = \sum_{k=1}^\infty (-1)^{k+m-1} k^{m-1} K_0(kl). \quad \text{(A.3)}$$

The summation (A.3) for $m = 2n+1$ can be evaluated by using the following formula [58],

$$\begin{aligned}
&\sum_{k=1}^\infty (-1)^k \cos(ka) K_0(kl) \\
&\quad = \frac{1}{2}\left(\gamma_E + \log\frac{l}{4\pi}\right) + \frac{\pi}{2}\sum_{j=1}^\infty \left[\frac{1}{\sqrt{l^2+[(2j-1)\pi - a]^2}} - \frac{1}{2\pi j}\right] \\
&\qquad\qquad + \frac{\pi}{2}\sum_{j=1}^\infty \left[\frac{1}{\sqrt{l^2+[(2j-1)\pi + a]^2}} - \frac{1}{2\pi j}\right]. \qquad \text{(A.4)}
\end{aligned}$$

For example,

$$\Phi_3^{(3)}(l) = -\pi \sum_{j=1}^\infty \frac{-l^2 + 2(2j-1)^2\pi^2}{[l^2+(2j-1)^2\pi^2]^{5/2}}, \quad \text{(A.5)}$$

$$\Phi_5^{(5)}(l) = 3\pi \sum_{j=1}^\infty \frac{3l^4 - 24(2j-1)^2\pi^2 l^2 + 8(2j-1)^4\pi^4}{[l^2+(2j-1)^2\pi^2]^{9/2}}. \quad \text{(A.6)}$$

By integrating both sides in (A.5), (A.6) etc., we find the general structure

$$\Phi'_{2n+1}(l) = \sum_{j=1}^{2n} \frac{\Phi_{2n+1}^{(j)}(0)}{(j-1)!} l^{j-1} + (-1)^n \pi \sum_{j=1}^\infty \frac{l^{2n}}{(2j-1)^{2n}\pi^{2n}\sqrt{l^2+(2j-1)^2\pi^2}}. \quad \text{(A.7)}$$

One can explicitly check this for small n's. Therefore

$$\begin{aligned}
\Phi_{2n+1}(l) &= \sum_{j=0}^{2n} \frac{\Phi_{2n+1}^{(j)}(0)}{j!} l^j \\
&\quad + (-1)^n \pi \sum_{m=n}^\infty \binom{-\frac{1}{2}}{m-n} \left(1 - \frac{1}{2^{2m+1}}\right) \zeta(2m+1) \frac{1}{2m+1} \left(\frac{l}{\pi}\right)^{2m+1}. \qquad \text{(A.8)}
\end{aligned}$$

The remaining task is to determine $\Phi_{2n+1}^{(j)}(0)$ $(j = 0, 1, \ldots, 2n)$. If we define $f(x) = \log(1 + e^{-x})$, from (A.2) we find

$$\Phi_{2n+1}^{(j)}(0) = f^{(j)}(0) \int_0^\infty \frac{dt}{\cosh^{2n-j+1} t} = \frac{2^{2n-j-1}\Gamma(n - \frac{j-1}{2})^2}{\Gamma(2n-j+1)} f^{(j)}(0). \tag{A.9}$$

From the following series expansion,

$$\log\cosh\frac{x}{2} = \sum_{j=2}^{\infty} \frac{(2^j - 1)B_j}{j! \cdot j} x^j, \tag{A.10}$$

we get

$$f(0) = \log 2, \qquad f^{(j)}(0) = \frac{(2^j - 1)B_j}{j} \ \ (j \geq 1), \tag{A.11}$$

where the Bernoulli numbers are defined by

$$\frac{x}{e^x - 1} = \sum_{n=0}^{\infty} \frac{B_n}{n!} x^n. \tag{A.12}$$

Substituting (A.9) and (A.11) into (A.8), we obtain the expansion of $\Phi_{2n+1}(l)$. In summary, the expansions of $\Phi_{2n+1}(l)$ are

$$\begin{aligned}\Phi_1(l) = {} & \frac{\pi}{2}\log 2 - \frac{l}{2}\left(\log\frac{1}{l} + 1 + \log\pi - \gamma_{\mathrm{E}}\right) \\ & + \pi \sum_{m=1}^{\infty} \binom{-\frac{1}{2}}{m} \left(1 - \frac{1}{2^{2m+1}}\right) \zeta(2m+1) \frac{1}{2m+1} \left(\frac{l}{\pi}\right)^{2m+1},\end{aligned} \tag{A.13}$$

$$\begin{aligned}\Phi_{2n+1}(l) = {} & \frac{2^{2n-1}\Gamma(n+\frac{1}{2})^2}{\Gamma(2n+1)}\log 2 + \sum_{j=1}^{2n} \frac{2^{2n-1}(1-2^{-j})}{j \cdot j!} \frac{\Gamma(n - \frac{j-1}{2})^2 B_j}{\Gamma(2n-j+1)} l^j \\ & + (-1)^n \pi \sum_{m=n}^{\infty} \binom{-\frac{1}{2}}{m-n} \left(1 - \frac{1}{2^{2m+1}}\right) \zeta(2m+1) \frac{1}{2m+1} \left(\frac{l}{\pi}\right)^{2m+1}.\end{aligned} \tag{A.14}$$

Substituting (A.13) and (A.14) into (A.1), we obtain

$$F(l,\varphi) = \frac{1}{2}\log 2 - \frac{l}{2\pi}\left[\cos\varphi\left(\log\frac{1}{l} + 1 + \log\pi - \gamma_{\mathrm{E}}\right) + \varphi\sin\varphi\right] + \sum_{p=2}^{\infty} c_p(\varphi) l^p. \tag{A.15}$$

The expressions of $c_p(\varphi)$ are given by

$$
\begin{aligned}
&c_{2k}(\varphi) = \frac{(2^{2k}-1)B_{2k}}{4k(2k)!}\sin^{2k}\varphi, \\
&c_{2k+1}(\varphi) \\
&= \frac{\cos\varphi}{\pi}\sum_{n=0}^{k}\sin^{2n}\varphi\cdot(-1)^n\pi\binom{-\frac{1}{2}}{k-n}\left(1-\frac{1}{2^{2k+1}}\right)\zeta(2k+1)\frac{1}{2k+1}\frac{1}{\pi^{2k+1}} \\
&= \binom{-\frac{1}{2}}{k}\frac{1}{(2k+1)\pi^{2k+1}}\left(1-\frac{1}{2^{2k+1}}\right)\zeta(2k+1)\cos\varphi\ {}_2F_1(-k,1;\frac{1}{2}-k;\sin^2\varphi).
\end{aligned}
\tag{A.16}
$$

Note that the sum over even p can be performed,

$$
\sum_{k=1}^{\infty}c_{2k}(\varphi)l^{2k} = \frac{1}{4}\left(l\sin\varphi + 2\log\frac{1+e^{-l\sin\varphi}}{2}\right). \tag{A.17}
$$

Thus we finally arrive at the expansion (5.11).

B. Perturbation of the $(\mathbf{SU(2)_{-1/2}\times SU(2)_1})/\mathbf{SU(2)_{1/2}}$ coset model

In this appendix, we compute the high-temperature expansion of the free energy in the non-unitary $(\mathrm{SU}(2)_{-1/2}\times\mathrm{SU}(2)_1)/\mathrm{SU}(2)_{1/2}$ coset model perturbed by the primary field $\phi_{1,1,3}$ with dimension $\Delta=\bar{\Delta}=1/5$. This model plays an important role in analyzing the remainder function for the decagon with $M_1=M_2$. This model is equivalent to the non-unitary minimal model $\mathcal{M}_{3,5}$ perturbed by the relevant operator $\Phi=\Phi_{1,3}$, whose action takes the following form,

$$
S = S_{\mathrm{CFT}} + \hat{\lambda}\int d^2x\,\Phi(x). \tag{B.1}
$$

Using the result in [38], we can write down the coupling-mass relation

$$
\begin{aligned}
&\hat{\lambda} = \hat{\kappa}M^{8/5}, \\
&\hat{\kappa}^2 = \frac{1}{\pi^2}\gamma\left(-\frac{1}{5}\right)\gamma\left(\frac{3}{5}\right)\left[\frac{\sqrt{\pi}}{8}\gamma\left(\frac{1}{4}\right)\right]^{16/5}.
\end{aligned}
\tag{B.2}
$$

Note that $\hat{\kappa}$ is purely imaginary in this case as well as in the scaling Lee-Yang model $\mathcal{M}_{2,5}$. The central charge of the UV CFT is $c=-3/5$, and the ground state corresponds to the operator $\Phi_{1,2}$ with dimension $\Delta_0=\bar{\Delta}_0=-1/20$. Thus the effective central charge is given by

$$
\hat{c} = c - 12(\Delta_0+\bar{\Delta}_0) = \frac{3}{5}, \tag{B.3}
$$

which is one-half of the central charge for the $SU(3)_2/U(1)^2$ coset CFT as expected.

Let us consider the free energy of this model. Near the high-temperature limit $l \to 0$, the free energy is expanded as

$$\hat{F}(l) = \frac{\pi}{6}\hat{c} + \frac{1}{4}l^2 + \sum_{n=1}^{\infty} \hat{f}^{(n)} l^{8n/5}. \tag{B.4}$$

where

$$\hat{f}^{(n)} = \frac{\pi}{6}\hat{\kappa}^n \hat{C}^{(n)}, \tag{B.5}$$

$$\hat{C}^{(n)} = 12\frac{(-1)^n}{n!}(2\pi)^{2\Delta-1} \int \prod_{j=1}^{n-1} \frac{d^2 z_j}{(2\pi|z_j|)^{2(1-\Delta)}} \times \langle \Phi_0(\infty,\infty)\Phi(1,1)\Phi(z_1,\bar{z}_1)\cdots\Phi(z_{n-1},\bar{z}_{n-1})\Phi_0(0,0)\rangle_{\text{connected}}. \tag{B.6}$$

Recall that the vacuum operator is $\Phi_0 = \Phi_{1,2}$ and the perturbing operator is $\Phi = \Phi_{1,3}$. The first non-vanishing coefficient is $\hat{C}^{(1)}$:

$$\hat{C}^{(1)} = -12(2\pi)^{-3/5} C_{\Phi_0\Phi\Phi_0}, \tag{B.7}$$

where $C_{\Phi_0\Phi\Phi_0}$ is the structure constant, which was computed in [59],

$$(C_{\Phi_0\Phi\Phi_0})^2 = (D^{(1,2)}_{(1,3)(1,2)})^2 = \gamma\left(-\frac{1}{5}\right)\gamma\left(\frac{3}{5}\right)\gamma\left(\frac{4}{5}\right)^2. \tag{B.8}$$

Thus the leading correction is

$$\hat{f}^{(1)} = \frac{1}{16}\left(\frac{\pi}{4}\right)^{1/5}\gamma\left(\frac{1}{4}\right)^{8/5}\gamma\left(-\frac{1}{5}\right)\gamma\left(\frac{3}{5}\right)\gamma\left(\frac{4}{5}\right). \tag{B.9}$$

Returning to the discussion on the decagon, we obtain an expansion of the free energy with $M_1 = M_2 = M$,

$$A^{\text{decagon}}_{\text{free}}|_{M_1=M_2} = 2\hat{F}(l) = \frac{\pi}{5} + \frac{1}{2}l^2 + 2\hat{f}^{(1)}l^{8/5} + \cdots. \tag{B.10}$$

C. Generalization to complex masses

Here we discuss how to extend the expansions of the Y-functions to the case with complex masses. We focus on the decagonal case $\tilde{n} = 5$. However the generalization to $\tilde{n} \geq 6$ is straightforward.

Let us consider the expansion of the Y-functions. From the quasi-periodicity (4.21) and analyticity, the Y-functions should have the following expansion [11]

$$Y_j(\theta) = \frac{1}{2}\sum_{k=-\infty}^{\infty} Y_j^{(k)} e^{\frac{2k\theta}{5}}, \tag{C.1}$$

with $Y_2^{(k)} = (-1)^k Y_1^{(k)}$. In addition, the reality condition (2.11) constrains the coefficients as $Y_j^{(-k)} = \overline{Y_j^{(k)}}$, which gives

$$
\begin{aligned}
Y_1(\theta) &= \frac{1}{2}\sum_{k=0}^{\infty}\Big(Y^{(k)}e^{\frac{2k}{5}\theta} + \overline{Y^{(k)}}e^{-\frac{2k}{5}\theta}\Big)\,, \\
Y_2(\theta) &= \frac{1}{2}\sum_{k=0}^{\infty}(-1)^k\Big(Y^{(k)}e^{\frac{2k}{5}\theta} + \overline{Y^{(k)}}e^{-\frac{2k}{5}\theta}\Big)\,.
\end{aligned}
\tag{C.2}
$$

The coefficients $Y^{(k)}$ are functions of m_j and $\bar{m}_j$, and $Y^{(2)}$ here coincides with (6.25) if all the masses are real. $Y^{(k)}$ are expanded in powers of $l^{2/5}$, with the leading behavior $Y^{(k)} \sim l^{2k/5}$ for small l [11, 46]. Moreover, according to [40], this leading behavior is thought of as coming from the boundary perturbation in (4.16). The form of the expansion (4.16) then implies that the subleading corrections are given in powers of $l^{4/5}$. Thus, one may have

$$
Y^{(k)} = \sum_{p=0}^{\infty} b_{k,2p}\, l^{\frac{2}{5}(k+2p)}\,,
\tag{C.3}
$$

where $l = ML$ and M is an overall mass scale. This is in accord with the double expansion in terms of $le^{\pm\theta}$ discussed in [46]. At low orders, the absence of terms of order $l^{2(k+p')/5}$ with odd p' is also confirmed from the Y-system by following [34]. We have checked that the above expansion is consistent with numerical results.

It is convenient here to write the first few terms of the expansion of $Y_1(\theta)$ in $l^{2/5}$,

$$
2Y_1(\theta) = 2b_{00} + (b_{20}e^{\frac{4\theta}{5}} + \bar{b}_{20}e^{-\frac{4\theta}{5}})l^{4/5} + \mathcal{O}(l^{6/5}),
\tag{C.4}
$$

where we have used the fact that $b_{00} = \bar{b}_{00} = 2\cos(\pi/5)$ and $b_{10} = b_{02} = b_{12} = 0$ as seen in Appendix D. The coefficients $b_{k,2p}$ depend on both $\tilde{M}_j e^{-i\varphi_j}$ and $\tilde{M}_j e^{i\varphi_j}$ in general. It is important to notice that from (2.17) the TBA equations for $Y_j(\theta) = \tilde{Y}_j(\theta - i\varphi_j)$ are given by

$$
\log Y_j(\theta) = -\frac{1}{2}(\bar{m}_j e^{\theta} + m_j e^{-\theta}) + K * \log(1+Y_{j-1})(1+Y_{j+1}).
\tag{C.5}
$$

In order to reveal the complex mass dependence of $b_{k,2n}$, we consider the decoupling limit (chiral limit) $l \to 0$. In this limit, the new functions $Y_j^{\mathrm{kink}}(\theta) = Y_j(\theta - \log(l/2))$ satisfy the kink TBA equations (see [12] for example)

$$
\log Y_j^{\mathrm{kink}}(\theta) = -\tilde{M}_j e^{-i\varphi_j}e^{\theta} + K * \log(1+Y_{j-1}^{\mathrm{kink}})(1+Y_{j+1}^{\mathrm{kink}}).
\tag{C.6}
$$

From the periodicity, $Y_j^{\text{kink}}(\theta)$ have the expansion,

$$Y_j^{\text{kink}}(\theta) = \frac{1}{2}\sum_{k=0}^{\infty} Y_j^{\text{kink}(k)} e^{\frac{2k\theta}{5}}. \tag{C.7}$$

(C.6) suggests that the coefficients $Y_j^{\text{kink}(k)}$ are functions of $\tilde{M}_j e^{-i\varphi_j}$, not of $\tilde{M}_j e^{i\varphi_j}$. On the other hand, by taking the decoupling limit in (C.2) with (C.3), we obtain

$$Y_1^{\text{kink}}(\theta) = \lim_{l\to 0} Y_1\left(\theta - \log\frac{l}{2}\right) = b_{00} + \frac{1}{2}\sum_{k=0}^{\infty} 2^{\frac{2k}{5}} b_{k0} e^{\frac{2k\theta}{5}}. \tag{C.8}$$

Comparing (C.8) with (C.7), we obtain

$$Y_1^{\text{kink}(0)} = 2b_{00}, \quad Y_1^{\text{kink}(k)} = 2^{2k/5} b_{k0}. \tag{C.9}$$

These relations show that the coefficients b_{k0} $(k \geq 1)$ depend on $\tilde{M}_j e^{-i\varphi_j}$, not on $\tilde{M}_j e^{i\varphi_j}$. Similarly, $\bar{b}_{k0}$ $(k \geq 1)$ are functions of $\tilde{M}_j e^{i\varphi_j}$. In summary, we can get b_{k0} $(\bar{b}_{k0})$ for the complex masses by replacing $\tilde{M}_j \to \tilde{M}_j e^{-i\varphi_j}$ $(\tilde{M}_j e^{i\varphi_j})$ in b_{k0} for the real masses assuming the analyticity in $\tilde{M}_j$. However, $b_{k,2n}$ $(n \geq 1)$ are functions of $\tilde{M}_j e^{-i\varphi_j}$ and $\tilde{M}_j e^{i\varphi_j}$, and the above argument does not applied to them. We already know the small l expansion of the Y-functions for the real masses up to order $l^{4/5}$ (see (6.23)). The coefficient of $l^{4/5}$ is

$$b_{20}^{\text{real}} = Y^{(2)}(\tilde{M}_1, \tilde{M}_2). \tag{C.10}$$

Using this result, we can obtain b_{20} and $\bar{b}_{20}$ for the complex masses by the above prescription,

$$b_{20}^{\text{complex}} = Y^{(2)}(\tilde{M}_1 e^{-i\varphi_1}, \tilde{M}_2 e^{-i\varphi_2}), \tag{C.11}$$

$$\bar{b}_{20}^{\text{complex}} = Y^{(2)}(\tilde{M}_1 e^{i\varphi_1}, \tilde{M}_2 e^{i\varphi_2}). \tag{C.12}$$

Substituting these equations into (C.4), we obtain the small l expansion of the Y-functions for the complex masses as in (6.40).

D. Structure of expansions at higher orders

In the main text, we have obtained the first order high-temperature expansion of the Y-functions for the decagon by using the conformal perturbation. In this appendix, we show that the structure of the high-temperature expansion is largely constrained by the Y-system, the structure of the conformal perturbation, and the symmetries

associated with the space-time parity and cyclicity, although one still needs higher order perturbations to find precise values of the coefficients. In the following, we concentrate on the case of the AdS_3 decagon, but the discussion below can be extended to more general cases.

We start with the expansion (C.2), and (C.3) which is in accord with the conformal perturbation as discussed in Appendix C. Substituting these into the Y-system (2.10) for the AdS_3 decagon, one obtains a double expansion in $e^{2\theta/5}$ and $l^{2/5}$, in which each coefficient should vanish. For the first few orders, we then find, e.g.,

$$\begin{aligned} &b_{00} = 2\cos\big(\frac{\pi}{5}\big)\,, \quad b_{10} = b_{02} = b_{12} = 0\,, \\ &b_{04} = \frac{1}{5}\sin^2\big(\frac{2\pi}{5}\big)\cdot b_{20}\bar{b}_{20}\,, \quad b_{40} = \frac{2}{5}\sin^2\big(\frac{\pi}{5}\big)\cdot (b_{20})^2\,. \end{aligned} \tag{D.1}$$

The expansion of the Y-functions in turn gives the expansions of the cross-ratios and $\Delta A_{\rm BDS}$. Using the relations among $b_{k,2p}$ obtained from the Y-system, we find that

$$\Delta A_{\rm BDS} = \sum_{k=0}^{\infty} A_k l^{2k/5}\,, \tag{D.2}$$

with

$$\begin{aligned} &A_0 = -\frac{2}{5}\log^2\big(2\cos\frac{\pi}{5}\big)\,, \quad A_4 = B_2\cdot b_{20}\bar{b}_{20}\,, \\ &A_6 = B_2(b_{20}\bar{b}_{22} + b_{22}\bar{b}_{20} + b_{30}\bar{b}_{30}) - 40\cos^4\big(\frac{2}{5}\pi\big)\cdot b_{30}\bar{b}_{30}\,, \end{aligned} \tag{D.3}$$

and $A_1 = A_2 = A_3 = A_5 = A_7 = 0$. B_2 is given in (6.30). The result shows that one can obtain the expansion of $\Delta A_{\rm BDS}$ up to $\mathcal{O}(l^{12/5})$ once b_{20} is known. In the main text and Appendix C, b_{20} is found to be $b_{20} = Y^{(2)}\big(\tilde{M}_1 e^{-i\varphi_1}, \tilde{M}_2 e^{-i\varphi_2}\big)$.

One can argue that the absence of A_k with odd k is understood as a consequence of the $\mathbb{Z}_{10}$ symmetry due to the space-time parity and cyclicity, $x_i^- \to x_{i+1}^+, x_i^+ \to x_i^-$. The $\mathbb{Z}_{10}$ transformation is concisely expressed by the Y-functions as [21]

$$Y_j(\theta) \to Y_j\big(\theta + \frac{\pi}{2}i\big)\,, \tag{D.4}$$

or in terms of the expansion coefficients and the TBA masses, $Y^{(k)} \to e^{\frac{\pi i}{5}k}Y^{(k)}$ and $m_j \to m_j/i$, respectively. The cross-ratios $c_{13}^{\pm}, c_{14}^{\pm}$ transform as $c_{13}^- \to c_{24}^+$, $c_{14}^- \to c_{25}^+$, $c_{13}^+ \to c_{13}^-$, $c_{14}^+ \to c_{14}^-$, where c_{24}^+, c_{25}^+ are given in (6.7). $\Delta A_{\rm BDS}$ in (6.4) indeed has this symmetry. Note also that A_k consists of terms of the form $\prod b_{p_j,2q_j}\prod \bar{b}_{\bar{p}_j,2\bar{q}_j}$ with $k = \sum(p_j + 2q_j) + \sum(\bar{p}_j + 2\bar{q}_j)$, which transform under (D.4) as $\prod b_{p_j,2q_j}\prod \bar{b}_{\bar{p}_j,2\bar{q}_j} \to e^{\frac{\pi i}{5}\Delta p}\prod b_{p_j,2q_j}\prod \bar{b}_{\bar{p}_j,2\bar{q}_j}$ with $\Delta p := \sum p_j - \sum \bar{p}_j$. Thus, unless

non-trivial cancellations with other terms occur, which is unlikely because $b_{p,2q}$ are functions of $m_j, \bar{m}_j$, the terms with $\Delta p \neq 0 \pmod{10}$ are projected out by successive actions of the $\mathbb{Z}_{10}$ transformation. For odd k, Δp necessary becomes non-zero and hence A_k is projected out. This leads to the symmetry $l^{2/5} \to -l^{2/5}$. Furthermore, the $\mathbb{Z}_{10}$ symmetry is then promoted to a continuous symmetry $Y^{(k)} \to e^{i\phi k} Y^{(k)}$, which in turn corresponds to a continuous imaginary shift of θ in $Y_j(\theta)$ and hence the world-sheet rotational symmetry.

$\Delta A_{\rm BDS}$ is also invariant under the space-time parity symmetry: $x_i^+ \to x_i^-$ with the order of the labeling of the cusps being reversed. In the case of the decagon, this gives rise to $c_{13}^{\pm} \leftrightarrow c_{14}^{\pm}$, which is equivalent to $l^{2/5} \to -l^{2/5}$ and $Y^{(k)} \leftrightarrow \overline{Y^{(k)}}$. Combined with the above symmetry $l^{2/5} \to -l^{2/5}$, the parity results in the symmetry $Y^{(k)} \leftrightarrow \overline{Y^{(k)}}$. Consequently, only the terms with $\Delta p = 0$ and maintaining the symmetry $Y^{(k)} \leftrightarrow \overline{Y^{(k)}}$, such as $b_{p,2q}\bar{b}_{p,2q'} + \bar{b}_{p,2q} b_{p,2q'}$, are allowed in the expansion.

In addition, since the remainder function has to have the parity and $\mathbb{Z}_{10}$ symmetries, $A_{\rm period} + A_{\rm free} (= R_{10} - \Delta A_{\rm BDS})$ also maintains these symmetries. Oppositely, since $A_{\rm period} + A_{\rm free}$ is invariant under the world-sheet rotational symmetry by definition, so is the remainder function.

Regarding the functional form of $b_{p,2q}$, the conformal perturbation and the expansion in $le^{\pm\theta}$ [46] for complex TBA masses suggest that $b_{p,2q}$ are given by summation of terms of the from $l^{-\frac{2}{5}(p+2q)} \bar{m}_{j_1}^{2/5} \cdots \bar{m}_{j_{p+q}}^{2/5} \cdot m_{j_1'}^{2/5} \cdots m_{j_q'}^{2/5}$. Indeed, given this form, one finds that $Y^{(k)}$ transform as $Y^{(k)} \to e^{\frac{\pi i}{5} k} Y^{(k)}$ and $Y^{(k)} \to e^{-i\frac{2k}{5}\varphi} Y^{(k)}$ under the $\mathbb{Z}_{10}$ transformation $m_j \to m_j/i$ and the world-sheet rotation equivalent to $m_j \to e^{i\varphi} m_j$, respectively. This is in accord with (D.4) and the above argument. Note that the invariants under the latter symmetry depend on the phases of m_j only through their deference $\varphi_{12} = \varphi_1 - \varphi_2$.

Our results of the expansion are all consistent with the above arguments. However, further investigations are needed for definite conclusions.

We can also study the structure of the high-temperature expansion of the remainder function at two loops. From the expansion of $Y_j(\theta)$ in (C.2), (C.3), we find that the remainder function (7.10) is expanded as

$$R_{10}^{\text{2-loop}} = \sum_{k=0}^{\infty} R_{10}^{\text{2-loop}\,(k)} l^{2k/5}\,, \tag{D.5}$$

with

$$R_{10}^{\text{2-loop}\,(0)} = -\frac{\pi^4}{12} - 5\log^4\!\big(2\cos\frac{\pi}{5}\big)\,, \quad R_{10}^{\text{2-loop}\,(4)} = D_2 \cdot b_{20}\bar{b}_{20}\,, \tag{D.6}$$
$$R_{10}^{\text{2-loop}\,(6)} = D_2(b_{20}\bar{b}_{22} + b_{22}\bar{b}_{20} + b_{30}\bar{b}_{30}) + 5\cdot 2^8\cos^9\!\Big(\frac{2\pi}{5}\Big)\log^2\!\Big(2\cos\frac{\pi}{5}\Big)\cdot b_{30}\bar{b}_{30}\,,$$

and $R_{10}^{\text{2-loop}\,(1)} = R_{10}^{\text{2-loop}\,(2)} = R_{10}^{\text{2-loop}\,(3)} = R_{10}^{\text{2-loop}\,(5)} = R_{10}^{\text{2-loop}\,(7)} = 0$. D_2 is given in (7.14). Thus, the structure of the expansion is very similar to that of ΔA_{BDS}. This is because $R_{10}^{\text{2-loop}}$ has the parity and $\mathbb{Z}_{10}$ symmetries and hence the structure of the expansion is strongly constrained as in the case of ΔA_{BDS}.

References

[1] L. F. Alday and J. M. Maldacena, JHEP **0706** (2007) 064 [arXiv:0705.0303 [hep-th]].

[2] J.M. Drummond, G.P. Korchemsky and E. Sokatchev, Nucl. Phys. B **795** (2008) 385 [arXiv:0707.0243 [hep-th]].
A. Brandhuber, P. Heslop and G. Travaglini, Nucl. Phys. B **794** (2008) 231 [arXiv:0707.1153 [hep-th]].
J.M. Drummond, J. Henn, G.P. Korchemsky and E. Sokatchev, Nucl. Phys. B **795** (2008) 52 [arXiv:0709.2368 [hep-th]]; Nucl. Phys. B **826** (2010) 337 [arXiv:0712.1223 [hep-th]].

[3] L. F. Alday and J. Maldacena, JHEP **0711** (2007) 068 [arXiv:0710.1060 [hep-th]].

[4] J.M. Drummond, J. Henn, G.P. Korchemsky and E. Sokatchev, Nucl. Phys. B **815** (2009) 142 [arXiv:0803.1466 [hep-th]].
Z. Bern, L.J. Dixon, D.A. Kosower, R. Roiban, M. Spradlin, C. Vergu and A. Volovich, Phys. Rev. D **78** (2008) 045007 [arXiv:0803.1465[hep-th]].

[5] Z. Bern, L. J. Dixon and V. A. Smirnov, Phys. Rev. D **72** (2005) 085001 [arXiv:hep-th/0505205].

[6] L. F. Alday and J. Maldacena, JHEP **0911** (2009) 082 [arXiv:0904.0663 [hep-th]].

[7] L. F. Alday, D. Gaiotto and J. Maldacena, arXiv:0911.4708 [hep-th].

[8] L. F. Alday, J. Maldacena, A. Sever and P. Vieira, J. Phys. A **43** (2010) 485401 [arXiv:1002.2459 [hep-th]].

[9] Y. Hatsuda, K. Ito, K. Sakai and Y. Satoh, JHEP **1004** (2010) 108 [arXiv:1002.2941 [hep-th]].

[10] A. Kuniba, T. Nakanishi and J. Suzuki, arXiv:1010.1344 [hep-th].

[11] Al. B. Zamolodchikov, Phys. Lett. B **253** (1991) 391.

[12] Al. B. Zamolodchikov, Nucl. Phys. B **342** (1990) 695.

[13] Y. Hatsuda, K. Ito, K. Sakai and Y. Satoh, JHEP **1009** (2010) 064 [arXiv:1005.4487 [hep-th]].

[14] I. Affleck and A. W. W. Ludwig, Phys. Rev. Lett. **67** (1991) 161.

[15] P. Dorey, A. Lishman, C. Rim and R. Tateo, Nucl. Phys. B **744** (2006) 239 [arXiv:hep-th/0512337].

[16] P. Dorey, D. Fioravanti, C. Rim and R. Tateo, Nucl. Phys. B **696** (2004) 445 [arXiv:hep-th/0404014].

[17] C. R. Fernandez-Pousa, M. V. Gallas, T. J. Hollowood and J. L. Miramontes, Nucl. Phys. B **484** (1997) 609 [arXiv:hep-th/9606032].

[18] D. Gepner, Nucl. Phys. B **290** (1987) 10.

[19] V. Del Duca, C. Duhr and V. A. Smirnov, JHEP **1009** (2010) 015 [arXiv:1006.4127 [hep-th]].

[20] P. Heslop and V. V. Khoze, JHEP **1011** (2010) 035 [arXiv:1007.1805 [hep-th]].

[21] D. Gaiotto, J. Maldacena, A. Sever and P. Vieira, arXiv:1010.5009 [hep-th].

[22] J. Maldacena and A. Zhiboedov, JHEP **1011** (2010) 104 [arXiv:1009.1139 [hep-th]].

[23] I. Bakas, Int. J. Mod. Phys. A **9** (1994) 3443 [arXiv:hep-th/9310122].
Q. H. Park, Phys. Lett. B **328** (1994) 329 [arXiv:hep-th/9402038].
I. Bakas, Q. H. Park and H. J. Shin, Phys. Lett. B **372** (1996) 45 [arXiv:hep-th/9512030].

[24] D. Gepner and Z. Qiu, Nucl. Phys. B **285** (1987) 423.
V. A. Fateev and A. B. Zamolodchikov, Sov. Phys. JETP **62** (1985) 215 [Zh. Eksp. Teor. Fiz. **89** (1985) 380].

[25] Al. B. Zamolodchikov, Int. J. Mod. Phys. A **10** (1995) 1125.

[26] J. L. Miramontes and C. R. Fernandez-Pousa, Phys. Lett. B **472** (2000) 392 [arXiv:hep-th/9910218].

[27] O. A. Castro-Alvaredo and A. Fring, Phys. Rev. D **64** (2001) 085007 [arXiv:hep-th/0010262].

[28] O. A. Castro-Alvaredo, A. Fring, C. Korff and J. L. Miramontes, Nucl. Phys. B **575** (2000) 535 [arXiv:hep-th/9912196].

[29] P. Dorey and J. L. Miramontes, Nucl. Phys. B **697** (2004) 405 [arXiv:hep-th/0405275].

[30] I. V. Cherednik, Theor. Math. Phys. **61** (1984) 977 [Teor. Mat. Fiz. **61** (1984) 35].

[31] Al. B. Zamolodchikov, Nucl. Phys. B **358** (1991) 497.

[32] H. Itoyama and P. Moxhay, Phys. Rev. Lett. **65**, 2102 (1990).

[33] T. R. Klassen and E. Melzer, Nucl. Phys. B **350** (1991) 635.

[34] Al. B. Zamolodchikov, Nucl. Phys. B **358** (1991) 524.

[35] G. Mussardo, "Statistical Field Theory," Oxford Univ. Press, 2010.

[36] Al. B. Zamolodchikov, Nucl. Phys. B **366** (1991) 122.

[37] F. Ravanini, R. Tateo and A. Valleriani, Int. J. Mod. Phys. A **8** (1993) 1707 [arXiv:hep-th/9207040].

[38] V. A. Fateev, Phys. Lett. B **324** (1994) 45.

[39] V. V. Bazhanov, S. L. Lukyanov and A. B. Zamolodchikov, Commun. Math. Phys. **177** (1996) 381 [arXiv:hep-th/9412229].

[40] P. Dorey, I. Runkel, R. Tateo and G. Watts, Nucl. Phys. B **578** (2000) 85 [arXiv:hep-th/9909216].

[41] A. Fring and R. Koberle, Nucl. Phys. B **421** (1994) 159 [arXiv:hep-th/9304141].

[42] S. Ghoshal and A. B. Zamolodchikov, Int. J. Mod. Phys. A **9** (1994) 3841 [Erratum-ibid. A **9** (1994) 4353] [arXiv:hep-th/9306002].

[43] R. Sasaki, "Reflection Bootstrap equations for Toda field theory," in the proceedings of the conference, Interface between physics and mathematics, eds. W. Nahm and J.-M. Shen [arXiv:hep-th/9311027].

[44] B. Pozsgay, JHEP **1008** (2010) 090 [arXiv:1003.5542 [hep-th]].

[45] F. Woynarovich, arXiv:1007.1148 [cond-mat.str-el].

[46] P. Dorey and R. Tateo, Nucl. Phys. B **515** (1998) 575 [arXiv:hep-th/9706140].

[47] V. G. Kac and D. H. Peterson, Adv. Math. **53** (1984) 125.
T. Gannon, arXiv:hep-th/0106123.

[48] A. N. Kirillov, Zap. Nauchn. Semin. Leningr. Otdel. Mat. Inst. **164** (1987) 121 [J. Math. Sci. **47** (1989) 2450].

[49] W. Nahm, A. Recknagel and M. Terhoeven, Mod. Phys. Lett. A **8** (1993) 1835 [arXiv:hep-th/9211034].

[50] A. LeClair, G. Mussardo, H. Saleur and S. Skorik, Nucl. Phys. B **453** (1995) 581 [arXiv:hep-th/9503227].

[51] R. Chatterjee, Nucl. Phys. B **468** (1996) 439 [arXiv:hep-th/9509071].

[52] A. Brandhuber, P. Heslop, V. V. Khoze and G. Travaglini, JHEP **1001** (2010) 050 [arXiv:0910.4898 [hep-th]].

[53] L. F. Alday, D. Gaiotto, J. Maldacena, A. Sever and P. Vieira, arXiv:1006.2788 [hep-th].

[54] J. Bartels, J. Kotanski and V. Schomerus, JHEP **1101** (2011) 096 [arXiv:1009.3938 [hep-th]].

[55] V. V. Bazhanov, S. L. Lukyanov and A. B. Zamolodchikov, Commun. Math. Phys. **190** (1997) 247 [arXiv:hep-th/9604044].

[56] V. V. Bazhanov, S. L. Lukyanov and A. B. Zamolodchikov, Nucl. Phys. B **489** (1997) 487 [arXiv:hep-th/9607099].

[57] D. Fioravanti and M. Rossi, JHEP **0308** (2003) 042 [arXiv:hep-th/0302220].

[58] I. S. Gradshteyn and I. M. Ryzhik, "Table of integrals, Series and Products," Fifth edition, Academic Press, 1980.

[59] V. S. Dotsenko and V. A. Fateev, Phys. Lett. B **154** (1985) 291.